

MOLECULE FORMATION IN AND ON GRAINS.I: PHYSICAL REGIMES

Amir Levinson¹

Astronomy Department, Cornell University

David F. Chernoff

Astronomy Department, Cornell University

Edwin E. Salpeter

Astronomy and Physics Department, Cornell University

We study molecular hydrogen formation in and on solids. We construct a model with surface sites and bulk sites capable of describing (1) the motion and exchange of H and H₂ between surface and bulk, (2) the recombination of H and dissociation of H₂ in and on the solid, and (3) the injection of H from the gas phase and the loss of H and H₂ from the solid. The basic physical processes include thermally activated reactions, collisionally induced reactions, and tunneling reactions.

Our main application is to the astronomical problem of H₂ formation on grains in space but the model has more general applicability. We investigate the steady-state H and H₂ concentrations in and on the solid when gas phase atoms or ions stick to the surface or penetrate the body of the grain. The model identifies ranges of physical parameters for which the solid becomes saturated (surface and/or bulk) with particles (H and/or H₂) and facilitates the calculation of the efficiency of molecule formation (the fraction of the gas phase atoms that leave as molecules). These solutions are highly degenerate in the sense that they depend only on a small number of dimensionless parameters. We find that a variety of recombination pathways operate under a broad range of conditions.

As an example we study H₂ formation in and on carbon grains. If molecules form from H on the surface by quantum tunneling *alone*, efficient transformation of incoming atoms takes place at grain temperatures less than 75 – 100 K for $1 < (n(\text{H})/\text{cm}^{-3})(\epsilon/\text{eV})^{1/2} < 10^7$ where $n(\text{H})$ and ϵ are the number density and energy of incident particles. When incident particles are energetic enough to penetrate the surface, the bulk of the grain will be saturated by H and/or H₂ under most circumstances. Additional molecule formation pathways (recombination on the surface or in the bulk) increase the efficiency of the transformation but only rapid bulk to surface exchange of H₂ can alter the conclusion regarding saturation. Saturation can lead to fundamental changes in the parameters that describe the grain.

I. INTRODUCTION

The interaction of hydrogen with solids is a topic of considerable interest in astrophysics, as well as other applied fields (materials research in fusion devices, thin film growth and surface etching of semiconductors, and adsorption and desorption reaction dynamics in catalysis). There is likewise a great deal of interest in exploring the fundamental physical processes that govern the interaction between gas atoms/ions and the solid surface/bulk. In this paper we develop a model to describe the behavior of H and H₂ in and on solids. The model is phenomenological – it identifies and parameterizes a set of reaction pathways thought to play important roles in determining the concentrations of H and H₂ in and on the solid.

Our main application is the study of efficiency of molecule formation on and release from astronomical grains. The possibility that grain surfaces catalyze the formation of H₂ inside cold atomic/molecular clouds has long been recognized². Under quiescent conditions, the chemisorption sites are filled and hydrogen is weakly bound by physical adsorption. In this scenario, low grain temperatures are necessary for the catalysis else the H atoms evaporate before they can recombine. The gas temperature must also be low else the neutral gas atoms rebound from the grain surface. Observations show that molecular hydrogen emission is excited during many phases of a star’s life. Well-studied regions include the Orion Molecular Cloud (Orion OMC-1, e.g. refs.^{3,4}, evolved supernova remnants (IC443⁵; Cygnus⁶), various Herbig-Haro objects (HH 7-11, e.g., refs.^{7,4}, Seyfert galactic nuclei (NGC1275⁸) and interacting starburst galaxies (NGC3690-IC694⁹). In each cited example the emission has been linked to shock heating, however, shock models often run into a common difficulty, finding a way to account for the emitting molecular hydrogen under decidedly non-quiescent conditions.

The main motivation is to explore new and different pathways for H₂ formation that may operate under more extreme conditions than hitherto considered, e.g. in the vicinity of a 100 km s⁻¹ shock. Several possibilities are of interest: (1) Energetic protons can penetrate the grain lattice and diffuse within. H can recombine within the grain or diffuse to the surface and recombine. (2) Energetic particles can drive endothermic molecule formation reactions and also eject and/or dissociate H containing species from the grain. (3) Energetic particles can sputter the surface and generate a large surface density of pits and edges, sites which can act as points of increased physical adsorption. We explore the important physical parameters that regulate molecule formation in the first two scenarios. These possibilities may turn out to be of astrophysical importance if they can provide means for rapidly reforming a small amount of molecular hydrogen in gas that has recently been shocked. If fast shocks radiate significantly more molecular line radiation than is currently thought, re-interpretation of a large body of work may be necessary.

Motivated by these considerations, we explore grain mediated molecule formation under a wide range of conditions including those that would be found in the vicinity of a shock. We describe the most important physical parameters, we review which parameters have been determined by laboratory experiments and astronomical observations, and we construct models that illustrate the different qualitative outcomes for molecule formation. Although our analysis is motivated primarily by astrophysical considerations, it is sufficiently general to be applied to other systems. For example, modeling high fluence hydrogen implantation in solids may follow the general strategy presented in this paper.

In §II we provide a brief overview of the typical energy barriers of interest in the formation pathways and, for comparison, the particle energy scales expected behind an astrophysical shock. We describe the typical grain temperature and note the wide range of grain composition and size with which we are concerned. In §III we outline the molecule formation pathways and identify key parameters. We briefly review the following topics: the transmission and reflection of incoming gas particles, the stopping ranges, the possible ordering of energy levels between the bulk, surface and vacuum, the H-H pairwise interaction in and on the solid, and the diffusion of H in and on the solid. Where necessary, we adopt a more or less phenomenological description of rate coefficients for the succeeding analysis. In §IV we formulate the model, including the basic equations and the conservation laws. We focus on a grain with one type of surface site and one type of bulk site. H₂ formation is calculated in three successively more general models: (i) pairwise recombination involving H₂ ejection from the surface, (ii) plus recombination and binding of H₂ on the surface, (iii) plus recombination and binding in the bulk. In §V we apply our results to graphite grains. In §VI we summarize.

II. CHARACTERISTIC POSTSHOCK ENERGY SCALES

Three key endothermic processes – ion implantation in the solid, sputtering of the surface atoms and chemical reactions driven by energetic particles – occur in the molecule formation pathways. As we discuss in more detail below, the threshold for implantation is expected to be ~ 10 eV, but has not been well-characterized for astrophysical grain material. The sputtering thresholds for H (He) range from $\sim 25 - 60$ eV ($\sim 10 - 16$ eV) for refractory grain

material (graphite, silicate and iron¹⁰). The strength of a typical H bond is 1 – 5 eV (chemical) or $\sim 0.05 - 0.5$ eV (physical absorption,¹¹). The equipartition thermal energy of particles behind a 100 km s⁻¹ shock is ~ 10 eV and several factors may increase the energy of gas-grain collisions. As the grains of size a interact with the plasma they typically acquire a negative charge $Q \approx -2.5akT/e^{12}$ (a number of important additional effects are noted in ref.¹³) so that protons strike grains with a total energy of ~ 35 eV. In addition, grains of sufficiently large size ($a \gtrsim 10^{-5}$ cm) are betatron accelerated behind a strong radiative shock to velocities $\sim 3v_s$, where v_s is the shock velocity¹³. From the shock front to the recombination region, the grains interact with H⁺, He⁺ and He⁺⁺ with typical energies from 1-300 eV. The characteristic timescale for the gas to cool to 10⁴ K is $t_{cool} \sim 2 \times 10^{10} v_s^{3.2} / n_0$ s¹⁴, where n_0 is the preshock H-nuclei density and $v_{s7} = v_s / 10^7$ cm s⁻¹.

Observations show that interstellar grains span a range in size at least as wide as $5 \times 10^{-7} < a < 2 \times 10^{-5}$ cm and have absorption/emission features typical of silicate (Si-O stretching and O-Si-O bending modes), graphite and hydrocarbons (C-H stretching modes)¹⁵.

The ratio of the grain temperature to the hydrogen binding energy is an essential parameter in all molecule formation schemes; it regulates the rate of thermally activated diffusion, recombination and evaporation of atoms and molecules from the surface. The grain temperature is largely governed by the balance of heating of Lyman-alpha radiation trapped in the vicinity of the shock front with cooling by infrared emission. Silicate grains reach $T_{gr} \approx 320\text{K} [(n_0/10^6)v_{s7}^3/a_{-5}]^{0.2}$ and the results for graphite grains are comparable¹⁴. Note that at low densities, T_{gr} is much less, e.g. $T_{gr} \approx 20\text{K} [n_0v_{s7}^3/a_{-5}]^{0.2}$ and quantum mechanical tunneling competes with the mechanism of thermal activation in the processes listed above.

III. KEY PARAMETERS

A. Outline for Molecule Formation

Here we provide a schematic overview of the formation mechanism:

1. H or H⁺ impinges on a grain; if H⁺, it is neutralized by electron transfer as it approaches.
2. A collision takes place and the atom rebounds, sticks or penetrates the surface. The lattice may be left intact, sputtered or damaged (i.e. defects introduced). If the grain surface includes H physically or chemically bound (X-H), then the incoming particle may drive a “pickup” reaction of the form X-H + H \rightarrow X + H₂.
3. Within the grain, the atom diffuses from site to site. It seeks out traps (vacancies, interstitials, etc.) where its binding energy is greatest. An equilibrium distribution is eventually formed in which the tightest binding sites are preferentially occupied.
4. When a new atom enters a grain it explores the grain interior by diffusion. Either it reaches the surface or it finds another atom, overcomes the activation barrier and forms H₂.
5. Bulk H₂ diffuses out of the grain, or remains in situ until it can escape directly. This is possible when damage of the lattice (by implantation, sputtering, radiation damage or grain-grain collisions) has accumulated to the point that passageways to the surface form.
6. If H₂ formation in the bulk is energetically unfavorable or inefficient, then the newly trapped atom diffuses to the surface where it recombines with another atom to form an H₂ molecule which immediately escapes from the grain. If the grain is too cold for surface recombination to proceed by thermal activation then quantum tunneling may allow recombination to proceed¹⁶.
7. In the case in which the ambient atoms are not energetic enough to penetrate the grain, the H₂ formation scenario suitable for cold clouds² takes place, but at possibly higher grain temperature and in the presence of enhanced binding sites (referred to as “semi chemisorption” in that paper). Atoms fill up the tightest binding sites, until the recombination rate plus the atom’s evaporation rate balances the flux of incoming particles.

The chemical network is governed by a number of key parameters: the mean interception time of H nuclei by the grain, the diffusion time of H and H₂ inside the grain, the surface and bulk binding energies for H and H₂ and the energy barriers for H₂ formation. In addition to normal sites in and on the grain, there are likely to be impurity sites whose number and characteristic binding energy for H and H₂ are important.

In the succeeding subsections we review some of the information relevant to the determination of these parameters and, ultimately, to our characterization of the rate coefficients for the model. In section IV, we examine in detail how the efficiency of molecular hydrogen formation depends on such quantities.

B. Transmission and Reflection of Low Energy Particles

At low energies ($E \lesssim 100$ eV) the *ab initio* calculation of the transmission and reflection coefficients of particles from a target surface is a formidable task. The results are of importance in plasma wall experiments, and such calculations have been the subject of many recent investigations^{17,18}. Many-body effects play an especially important role. Firstly, in contrast to the scattering of high-energy particles, which can be well approximated as a pure binary collision between the projectile and a surface atom, the scattering of low-energy particles involves simultaneous interaction with several nearby atoms, owing to the relatively long-range force between the ion and each surface atom (e.g., refs.¹⁹). As a result, the scattering of low energy ions is sensitive to the details of the ion-surface interaction potential. Secondly, in the case of scattering from metal surfaces, collective effects produce a significant attractive force, commonly represented as an image force^{19,20}, which plays a major role in determining the transmission coefficient at low energies.

Ignoring chemical reactions, there are three possible outcomes for a fast particle incident on a surface: the incident particle may stick to the surface of the target material, penetrate below the surface or reflect back into space. The typical energy at which each outcome is maximized varies with the incident ion and the target material. Masel²² reviews the status of trapping and sticking on solid surfaces. Baskes¹⁷ performed simulations of hydrogen reflection from a clean nickel surface, using the Embedded Atom Method to handle the many-body interactions in a self-consistent manner. For normal incidence, he found that the reflection coefficient peaks at an energy of order 6 eV where about 90% of the incident ions are reflected. Well above 6 eV the ions are energetic enough to penetrate the surface, and below it the ions are trapped, owing to the attractive image force which tends to increase the energy loss of the scattered ion to the surface. Similar theoretical results were obtained by Eckstein & Biersack¹⁸ who employed a modified TRIM code²¹ to calculate hydrogen reflection. They treated the surface binding energy as a free parameter and showed that at energies well above a few eV the reflection coefficient is independent of the surface potential, but at \lesssim a few eV, depending on the surface binding energy, becomes sensitive to it. In experiments similar behavior has been observed for scattering of Na^+ from Cu ²³.

Less is known about the reflection and sticking of H to non-metals. The sticking probability of atomic hydrogen on graphite at low (sub-eV) energies has been inferred from measurements to be at least a few percent²⁴. TRIM simulations¹⁸ of reflection of low energy H atoms from carbon give a maximum reflection coefficient smaller than from Ni and W, and a slightly higher energy at the maximum. These differences are mainly due to the difference in target mass. For a surface binding energy of 1 eV about 50% of the H atoms are found to be reflected from the carbon surface at the peak energy of 4 eV.

Let $T(E, a)$ be the fraction of incident particles that stick to or penetrate and do not exit a grain of size a at a given energy E . (Hence $T \sim 0$ for particles whose energy-dependent stopping range exceeds the grain size; equivalently, $T(E, a) \sim 0$ for $E > E_{max}(a)$ when E_{max} is the maximum energy particle stopped by the grain.) Let σ_g be the grain's geometric cross section for intercepting particles (including the focusing effect of Coulomb scattering), let \vec{v}_g be the grain's velocity and let $f(v)$ be the particle distribution function. Then the mean rate for particle interception by the grain is

$$t_{in}^{-1} = \int d^3v f(v) \sigma_g |\vec{v} - \vec{v}_g| T(E, a). \quad (1)$$

C. Stopping Ranges of Low Energy Ions in Solids

Energetic particles that penetrate into the grain will experience energy loss due to nuclear scattering and electronic stopping, i.e., energy transfer from the ion to the target nuclei and electrons (for a detailed account of the theory of ion stopping in solids see ref.²⁵). In order to be trapped inside the grain, the particle's stopping range must not exceed the characteristic grain size. At low energies, the stopping power is dominated by nuclear scattering²⁶ (see also refs.²⁹ for reviews on the stopping power of an electron gas).

The energy transferred in a pure binary collision from an incident projectile having energy E_0 and mass m , to a target particle of mass M , is

$$\Delta W = 4E_0 \frac{\mu}{(1 + \mu)^2} \sin^2 \frac{\theta}{2}, \quad (2)$$

where $\mu = m/M$ is the mass ratio, and θ is the center-of-mass scattering angle. The lab frame scattering angle, ψ , satisfies

$$\tan \psi = \frac{\sin \theta}{\cos \theta + \mu}. \quad (3)$$

For a proton scattering off heavy target nuclei ($\mu \ll 1$), Eq. 2 shows that the fraction of energy lost by the intruder in one collision is at most of order μ . Consequently, the number of collisions required to slow the incident proton from E_0 to final energy E_f will be $\sim \ln(E_0/E_f)/\mu$, and the corresponding stopping range, assuming that the ion undergoes a random walk with fixed step size, varies like $\mu^{-1/2}$. However, as already mentioned in §III B, at low energies, the scattering of an ion from an array of atoms is considerably more complicated than pure binary collision because the ion interacts simultaneously with several nearby atoms. This tends to increase the effective mass of the target object, thereby reducing the stopping power. Moreover, screening plays an important role at these energies and needs to be taken into account properly. Quantitative determination of range distributions requires numerical simulations²⁶. For our purposes, however, a rough upper limit on the average stopping range should suffice. For incident energies $E_0 < 100$ eV, final energy $E_f \sim 1$ eV, $\mu \sim 1/12$ (e.g. graphite grain), we estimate ≤ 70 collisions. If the mean free path is not greater than the lattice spacing then the stopping range of H will not exceed ~ 8 atomic layers. This upper limit is in agreement with recent experimental results reported in ref.²⁷.

We assume the grains are large enough to stop the particles that penetrate and we treat the system as a semi-infinite sample.

D. Energy Levels

The ground state energy of H and H₂ in the bulk, on the surface and in the vacuum are the fundamental parameters that govern the behavior of hydrogen with respect to solids. We denote the ground state energy of species X in the bulk, on the surface and in the vacuum as $E[X]^i$ where $i = b, s,$ and v respectively. For future use we define

- Chemisorption energy (for H) $E_c = E[\text{H}]^s - \frac{1}{2}E[\text{H}_2]^v$.
- Solution energy (for H) $E_s = E[\text{H}]^b - \frac{1}{2}E[\text{H}_2]^v$.
- Dissociation energy of H₂ (per nuclei) in bulk, on surface and in vacuum $E_d^i = E[\text{H}]^i - \frac{1}{2}E[\text{H}_2]^i$.
- Embedding energy (for H) $E_e = E[\text{H}]^v - E[\text{H}]^s$.

The most basic properties of the solid are governed by the signs and sizes of these energies. We adopt as the zero of the energy scale the level associated with H₂ in the vacuum, i.e. $E[\text{H}_2]^v = 0$, so it follows $E_d^v = 2.24$ eV. For an arbitrary grain there remain 4 quantities to specify. A simple counting shows that there are $3 \times 4 \times 5 \times 6 = 360$ possible orderings of the remaining levels, so it is impractical to consider separately all relative arrangements. Even for H levels alone, there exist $3 \times 4 = 12$ possible arrangements (relative orderings) of the levels in the bulk and on the surface. However, general arguments regarding H₂ formation and release highlight a much smaller group of relevant, distinct orderings. We discuss some of these below. Note that our method of computation (section IV) does not depend upon an assumed ordering. Further, it should be clear that in counting the distinct possibilities above, we have ignored many additional energy scales that can play important roles, such as the height of barriers for site-to-site migration within the bulk and the height of barriers for bulk-to-surface and surface-to-vacuum transitions in the potential energy curves.

1. H in bulk and surface; no H₂

We begin by reviewing the chemisorption and solution energy scales for H. These are of considerable interest in a number of areas, especially fusion research on plasma-surface interactions. New experimental and theoretical techniques have led to progress in understanding of the physics and quantitative calculation of the surface interaction^{28,22}. In many cases, the electronic wave function of the H atoms tends to form a chemical bond with the surface atoms, leading to a strong attractive force between the H atom and the solid surface as the atom approaches. For metals, the chemisorption sites are typically deeper than bulk sites (with the possible exception of deep trapping sites due to vacancies or defects). For semiconductors, bonds of a more local nature are formed and, for insulators, the situation is not well-understood²². In these cases and for graphite, the energy of chemisorption sites can lie above the energy of bulk sites.

Let us consider the possibilities when the H levels satisfy the inequality $\{E_c, E_s\} < E[\text{H}]^v$, which is typically the case for solids. The ordering implies that the surface and bulk ground states of H are energetically stable with respect

to H in the vacuum. The inequality drives the accumulation of H in or on the grain and the resultant high densities may promote H₂ formation by recombination from surface sites. Of course, H may escape by thermal evaporation, by collisional ejection or by molecule formation and subsequent ejection. If H and H₂ loss processes are slow then saturation occurs which will generally lead to changes in the solid's properties including energy levels. Given our assumptions above, there exist a total of 6 distinct level orderings.

For metals, it is typically the case that $E_c < E_s$ ³⁰ and the three possible 1D energy diagrams, shown in figure 1, have (i) $0 < E_c < E_s$, (ii) $E_c < 0 < E_s$ and (iii) $E_c < E_s < 0$. The solid line represents the schematic interaction potential of a single H atom with the solid. The figures illustrate the chemisorption energy E_c , solution energy E_s , and the vacuum dissociation energy of H₂ (per H) E_d^v . The two dashed lines represent half the energy of an H₂ pair at a given distance from the surface. One dashed line applies to a pair at fixed interatomic separation (equal to the bond length of a free H₂ molecule ~ 0.74 Å) and the other to the minimum energy configuration. The minimum energy configuration terminates near the surface where the pair separation becomes large. In general, the sign of the energy is defined by the direction of the corresponding arrow; positive if the arrow points upwards and negative if it points downwards.

It is observed that (e.g.³⁰, and references therein) as an energetic incoming H₂ molecule approaches the solid, it may dissociate into H atoms that are bound to the surface (with activation energy barrier per H of E_a); in the inverse process, pairs of H atoms on the surface may tunnel through or thermally ascend the energy barrier and recombine as H₂ (with recombination energy barrier per H of E_r). In figure 1 vertical bars without arrows represent manifestly positive quantities. We note that quantum pair recombination from the surface is allowed only in case (i). Surface recombination requires thermal activation in cases (ii-iii).^{*} In the case of metals, the embedding energy $E_e = E[\text{H}]^v - E_c$ typically lies in the range 2.4 to 2.8 eV³⁰, implying $E_c < 0$ [case(ii) or (iii)].

The situation for carbon and other non-metals is not as well characterized. Schermann et al.³¹ have reported the detection of H₂ formation by recombination of H atoms adsorbed on a carbon surface at temperatures between 90 and 300 K. The detected molecules appear to be in highly excited vibrational states. At zero temperature the measured vibrational states of the newly formed molecules constrain the embedding energy $E_e < 1$ eV for the H binding sites on the surface; consequently $E_c = E[\text{H}]^v - E_e > 1.24$ eV. The system is so cold that thermal effects cannot significantly change these estimates although there remains the possibility that H may bind to more than one type of surface site (for example, one physical and the other chemical). The solubility data implies $E_s < 0$ (see³² and references therein) so that $E_s < 0 < E_c$, illustrated as case (iv) in figure 1. It is plausible that recombination proceeds via quantum tunneling in this experiment. The possibility of quantum pair recombination may have important implications for H₂ formation and release which are considered below.

Two other orderings ($E_s < E_c < 0$ and $0 < E_s < E_c$) are possible but we are unaware of representative materials for which these cases would be relevant.

2. H and H₂ in bulk and surface

We now review what is known about the H pair interaction on the solid surface and in the bulk. It could be dramatically different than that in vacuum as it depends critically on many body interactions. For most metals as well as carbon, solubility data for hydrogen at sufficiently low bulk concentrations appear to follow Sieverts' law³³; that is, the bulk concentration of hydrogen is proportional to the square root of the equilibrium pressure. This implies that H₂ is not the preponderant state inside the solid, rather H (or one of its charged states) is. Some recent theoretical studies³⁴ have shown that the interaction between hydrogen atoms on metal surfaces and between atoms in surface and subsurface sites is repulsive and short-range with interaction energies of order 0.1 - 0.4 eV between atoms in nearest-neighbor sites. These facts hint that there is no bound state of H₂ in the bulk and/or that there are significant energy barriers that prevent the association of H to form H₂ in the bulk. The fact that Sieverts' law is satisfied even at very high temperatures in certain materials³⁵ suggests that energy barriers are not solely responsible. On the other hand, high fluence hydrogen implantation experiments in graphite and some amorphous carbon films³⁶ suggest that H₂ formation may take place in the bulk after becoming saturated. This observation is not decisive since other interpretations cannot be ruled out, particularly in view of the high porosity of these materials. And, in any case, the pair interaction in the solid is undoubtedly density dependent. At higher concentrations, the solid-hydrogen

^{*}Tunneling of a hydrogen pair from bulk to vacuum is energetically possible in cases (i-ii) but not (iii). However, in case (ii) the decay time to a surface site is likely to be very short and the corresponding transition rate negligibly small. Differences in H₂ formation between cases (i) and (ii) may be important but are unlikely to be influenced by the bulk-vacuum tunneling rate.

systems tend, in some cases³³, to undergo phase transitions to more ordered phases. We shall not consider such complications in the present analysis.

Given the great degree of uncertainty we regard the binding energy of H_2 in the bulk and on the surface as free parameters. For illustration, let us consider the possibility that there exist bound ground states of H_2 (for a not too large separation) in or on the solid. We adopt the inequality $\{E_c, E_s\} < E[H]^v$ discussed above for H. Furthermore, we consider only cases in which $E_d^b > 0$ and $E[H_2]^b > 0$ if H_2 levels exist in the bulk and similarly $E_d^s > 0$ and $E[H_2]^s > 0$ if H_2 levels exist on the surface. These inequalities imply that H_2 is energetically stable against dissociation in situ and that escape to the vacuum is energetically possible.

If the condition that H_2 be bound in situ (with respect to H) is not satisfied, the existence of metastable bound states may still be possible in principle. The lifetime of such states depends on the characteristics of the corresponding energy barriers and is accounted for by the analysis presented in §IV. And, even if the condition is satisfied dissociation will still occur due to thermal activation and collisions with injected atoms, as discussed in greater detail in §IV.

If the energy level of H_2 in the bulk and/or on the surface lies below that of H_2 in the vacuum, we may anticipate that the grain will become saturated with the molecules at sufficiently low temperatures.

For each of the previously discussed cases (i-iv) one can identify all the possibilities consistent with the general assumptions. Only case (i) with $0 < E_c < E_s$ allows H_2 levels *both in and on* the grain. (Case [ii] allows H_2 levels in but not on the solid, case [iv] on but not in, and [iii] neither.) Figure 2 illustrates one of three possible orderings for case (i). The thick arrows label different energetically allowed pathways for H_2 formation and release: H_2 formation in the bulk and on the surface, surface recombination, and evaporation of H_2 from the surface. Each reaction may involve an activation barrier with some characteristic height and width, as shown schematically in figure 2. The association pathways (labeled 1 and 2) depend upon the H-H pair potential in the bulk and on the surface. The pair recombination from the surface (either quantum mechanical or thermal, labeled 3) is identical to the pathway discussed in the previous section. The evaporation of H_2 from the surface is labeled 4.

We briefly review what is known about the association and dissociation kinematics of H_2 at the surface (i.e. paths 2 and 3 and inverses). Direct computations of these processes are difficult and involve multi-dimensional potential energy surfaces. They have been performed in a limited form for some hydrogen-metal systems^{37,38}. Molecular beam experiments as well as self-consistent many-body calculations indicate that for most metals there is an activation barrier for dissociation of width $\sim 0.6 \text{ \AA}$ about 2 \AA above the surface^{39,38}. For simple and noble metals the barrier ranges from about 0.2 eV (e.g., for Na) to more than 1 eV⁴⁰. The repulsive interaction between the molecule and the surface is due to the molecule being closed-shell, and is similar to the repulsion found for closed-shell atoms such as He as they approach the surface. However, in the case of an H_2 molecule the antibonding state is shifted downwards and gradually filled as it approaches closer to the surface, thereby leading to a weakening of the attractive H-H interaction and the ultimate dissociation of the H_2 molecule⁴¹. For transition metals (e.g, Ni, Pd) the activation barrier is appreciably smaller - about 0.05 to 0.1 eV - and for some systems (e.g., Ni(110)) the dissociation is non-activated. The reason for the small activation barrier observed in transition metals, as explained by Harris & Anderson⁴⁰, is that s electrons of the metal can occupy unfilled d states which are far more localized, thereby reducing the Pauli repulsion between the H_2 core electrons and metal electrons. Self-consistent calculations⁴¹ suggest that some metals may exhibit, in addition to the activation barrier of dissociation, a barrier for H_2 adsorption with a comparable height. Between the two barriers H_2 molecules can be trapped for a relatively long time, and this may account for the so-called molecular precursor state. For other materials there is no second barrier, but there is a small potential well just above the barrier due to van der Waals forces that can give rise to physisorption of H_2 molecules at very low ($< 20 \text{ K}$) temperatures³⁰. Large surface coverage seems to give rise to appreciably larger barriers, at least in the case of transition metals. For instance, the barrier for dissociation on a Ni(100) surface increases from 0.1 eV for a clean surface to about 0.6 eV for a surface with a full hydrogen monolayer coverage³⁸. Given these complications, we regard the activation barriers as parameters.

E. Diffusion of Hydrogen in Solids

Let the activation energies of diffusion of H and H_2 be E_{DH} and E_{DH_2} . Most theoretical and experimental studies of H diffusion in solids have focused on diffusion in metals. We briefly review what is known about diffusion in solids. At sufficiently high temperatures, the dependence of the diffusion coefficient on temperature is well described by the Arrhenius law:

$$D = D_o \exp(-E_{DH}/kT), \quad (4)$$

where the preexponential factor, D_o , is temperature independent. In the most rudimentary model of diffusion (for a review of the theory of diffusion of hydrogen in metals see e.g., ref.⁴²), the interstitial atom is supposed to be localized

at or about a given site. Diffusion occurs via a sequence of thermally activated jumps from one site to an adjacent one, in a random walk manner. The activation energy E_{DH} is connected, in this model, to the height of the potential barrier. The jump frequency is expected to be of order of the zero point frequency for harmonic oscillations of the atom around its equilibrium position, denoted here by ν_o . Letting ℓ denote the hopping length, the preexponential factor can be approximated as

$$D_o \simeq 10^{-3} q (\ell/\text{\AA})^2 (\nu_o/10^{13} \text{ s}^{-1}) \text{ cm}^2 \text{ s}^{-1}, \quad (5)$$

where q is a geometrical factor which depends on the lattice type.

The values of D_o and E_{DH} have been measured for some materials using various experimental techniques (for a review see ref.⁴³). For most metals, as well as for some nonmetals for which there are experimental data, D_o lies in the range 10^{-4} to a few times 10^{-2} $\text{cm}^2 \text{ s}^{-1}$, in accordance with Eq. (5). The activation energy appears to vary appreciably from one substance to another, ranging from about 0.043 eV for vanadium⁴³ to ~ 0.5 eV for titanium³². It should be noted that most of those measurements have been taken at relatively high temperatures and in a fairly narrow range. Moreover, for some materials (e.g., iron) there are quite large uncertainties, particularly at low temperatures. The determination of hydrogen diffusivity in carbon is difficult because of the presence of deep trapping sites that appear to control the mobility at low hydrogen concentrations; the diffusion energy inferred from experiments using low concentrations of hydrogen is about 4 eV, which is comparable with the trap energy. The best estimate of hydrogen diffusivity in graphite (when trapping sites are excluded) according to Causey⁴⁴ is $E_{DH} \simeq 2.8$ eV, $D_o \simeq 0.93 \text{ cm}^2 \text{ s}^{-1}$.

At low temperatures (~ 200 K for metals) quantum effects play a role, and deviations from the Arrhenius law are expected, and in some cases have been observed. (1) At extremely low temperatures, the interstitial eigenstates should fulfill Bloch's theorem and form a band. The diffusion process is then band propagation similar to electron conduction. The rate, limited by interaction with phonons and lattice defects, decreases as temperature rises. No indications of band propagation for hydrogen have been observed yet⁴². (2) At somewhat higher temperatures, the decay rate of the band states increases, and ultimately approaches the band width. As a consequence, at temperatures larger than some critical temperature the interstitial will be localized about a specific site, as discussed above. In this temperature regime, overbarrier transitions in the manner described above are negligible, and thermally activated tunneling from one site to another may dominate the diffusion process. In the small polaron theory⁴² one treats the tunneling matrix element as a small perturbation in the total Hamiltonian. It is then possible to compute the transition rate (i.e., hopping frequency) using time-dependent perturbation theory⁴². The results of such calculations show that well below the Debye temperature the transition rate should satisfy a T^7 law, which has not yet been verified experimentally. At temperatures greater than the Debye temperature, the transition rate obeys the Arrhenius law with an activation energy that corresponds to the energy difference between an occupied site and a vacant site (note that the slope of the $\log D$ vs. $1/T$ curve is different than that in the high temperature regime where overbarrier transitions dominate) and a preexponential factor that involves the tunneling matrix element (and therefore should be strongly isotope dependent).

From the foregoing discussion it is expected that at sufficiently low temperatures the diffusion coefficient will generally have non-exponential temperature dependence. The temperature at which this happens depends on the width of the potential barrier and other details of the interaction of the H atom with the lattice. Unfortunately, measurements of the diffusion coefficient at low temperatures are extremely difficult, and the value of D below about 200 K is poorly known.

The mobility of hydrogen on surfaces is some 10 - 15 orders of magnitudes larger than that in the bulk by virtue of the small barriers between surface sites. Recent measurements indicate that there is indeed a sharp transition for surface diffusion from a high temperature regime, wherein D obeys the Arrhenius law, to a low temperature regime, where D is essentially temperature independent. For example for W(110) at zero coverage this transition occurs at ~ 150 K⁴⁵. However, there is evidence for a strong anomalous isotope effect, as well as some other complications, which are not well understood at present.

At high concentrations, hydrogen diffusion in the solid may be altered significantly, owing to the increasing strength of the self interaction between the hydrogen atoms.

In view of the large uncertainty in D referred to above, we shall treat the mean hopping time between bulk sites, defined as $t_h = \ell^2/D$, as a free parameter.

IV. A MODEL OF MOLECULAR HYDROGEN FORMATION IN GRAINS

A. Basic Equations

We distinguish sites according to whether they lie in the bulk or on the surface of the solid and whether they are elements of the regular solid (“clean” sites) or correspond to centers of altered binding (impurities, vacancies, and defects collectively called “impurities”). In our model a site may be empty (ϕ), occupied by a single H with energy $E[\text{H}]$ or occupied by H_2 with energy $E[\text{H}_2]$; we do not allow multiple occupancy or excited energy levels. Denote by $\rho_{a\alpha}(\vec{x}, t)$ the number density of bulk sites of type a (a refers to clean bulk sites or to impurity sites of type k denoted I_k) that are occupied by species α ($\alpha = \text{H}, \text{H}_2$) at position \vec{x} at time t . Similarly, denote by $\sigma_{a\alpha}(\vec{x}, t)$ the corresponding areal number density of surface sites.

We assume that the average number of H and/or H_2 per grain is much larger than 1 so that rates of relevant binary reactions can be meaningfully expressed in terms of the average number densities of the reactants.

We assume that species diffuse in the bulk and along the surface of the grain and that exchange occurs between the gas phase, the solid bulk and the surface. We express the rate of change of the number densities by the following coupled set of equations:

$$\begin{aligned} \frac{\partial \rho_{a\alpha}}{\partial t} - \nabla(D_{a\alpha} \nabla \rho_{a\alpha}) &= \dot{\rho}_{a\alpha}, \\ \frac{\partial \sigma_{a\alpha}}{\partial t} - \nabla_s(D_{a\alpha}^s \nabla_s \sigma_{a\alpha}) &= \dot{\sigma}_{a\alpha}, \end{aligned} \quad (6)$$

where $D_{a\alpha}$ and $D_{a\alpha}^s$ are the bulk and surface diffusion coefficients, respectively, and ∇_s denotes gradient along the surface. The terms on the right hand side give the rate of change of density from external sources (we denote for future use the injection from the gas phase of species α into sites of type a in the bulk and on the surface by $s_{a\alpha}$ and $\hat{s}_{a\alpha}$, respectively) and from internal rearrangements of site occupancies. Internal changes in the bulk number densities occur from (i) *chemical reactions* taking place between bulk species or between bulk and surface species, (ii) *particle exchanges* between bulk and surface sites, and (iii) *particle losses* to the vacuum (either via evaporation or recombination). Rate coefficients for these processes depend on the parameters of the grain (temperature, energy levels, and so forth, including occupation probability).

Let $\delta_\alpha = (1, 2)$ for $\alpha = (\text{H}, \text{H}_2)$. Summing eqs. (6) over the entire grain, over all species and filled sites yields the total rate of change of hydrogen nuclei

$$\begin{aligned} \frac{d}{dt} \left\{ \sum_{a\alpha} \delta_\alpha \left(\int \rho_{a\alpha} dV + \int \sigma_{a\alpha} dS \right) \right\} = \\ t_{in}^{-1} - t_{H-out}^{-1} - 2t_{H_2-out}^{-1} \end{aligned} \quad (7)$$

where t_{in}^{-1} is the rate for atoms to strike the grain (eq. 1), t_{H-out}^{-1} is the loss rate of atoms and $t_{H_2-out}^{-1}$ is the loss rate of molecules. The loss terms include loss by evaporation (thermally and quantum mechanically), loss induced by fast collisions (direct ejections, pickup reactions, enhanced recombinations) and loss by pair recombination (thermally and quantum mechanically). In steady-state the flux of atoms intercepted by the grain is balanced by the total loss rate of atoms and molecules. Efficient molecule formation requires the total loss rate of molecules by all channels to exceed that of atoms. The relevant rates depend on the occupation numbers of the different species, which are determined by the various physical processes taking place in and on the grain. Below we explore the solutions to the above equations in different regimes of the parameter space, and elucidate the conditions under which effective molecular formation may take place.

In the examples presented below, we further assume that the occupation numbers are homogeneous within the bulk and homogeneous on the surface and that the grain temperature T_g is uniform throughout. In other words, we describe the chemical distribution in terms of two zones (bulk and surface). This approximation is justified whenever the diffusion timescale is short compared to all other characteristic timescales (for example, the injection time) and may also be reasonable under less restrictive conditions (for example, if the injection process is homogeneous). We define the total number of grain sites on the surface and in the bulk (occupied α or empty ϕ)

$$\mathcal{N} = \sum_{a,\alpha,\phi} \left(\int \rho_{a\alpha} dV + \int \sigma_{a\alpha} dA \right), \quad (8)$$

the fraction of \mathcal{N} that are in the bulk, of type a , and occupied by species α

$$n_{a\alpha} = \mathcal{N}^{-1} \int \rho_{a\alpha} dV, \quad (9)$$

the fraction of \mathcal{N} that are on the surface, of type a, and occupied by species α

$$\theta_{a\alpha} = \mathcal{N}^{-1} \int \sigma_{a\alpha} dA, \quad (10)$$

and the bulk and surface injection rates

$$S_{a\alpha} = \mathcal{N}^{-1} \int s_{a\alpha} dV \quad (11)$$

$$\mathcal{S}_{a\alpha} = \mathcal{N}^{-1} \int \hat{s}_{a\alpha} dA. \quad (12)$$

Steady state solutions are obtained by numerically integrating the time dependent rate equations (6) (integrated over the appropriate zone) until equilibrium is achieved. For the specific contributions we have included forward and backward reactions related by detailed balance for each process that involves thermalized surface and bulk reactants. For reactions driven by impinging fast particles and for particle loss to the vacuum we have included only the pathway of interest. We have not included any direct bulk to vacuum loss rates even when quantum tunneling might be possible.

Our analysis becomes inapplicable when the mean residence time of an hydrogen atom in the grain, Δt becomes much shorter than t_{in} . In this case the probability of finding two atoms simultaneously inside the grain is approximately $\Delta t/t_{in}$, assuming that injection of atoms is a Poisson process. Consequently, even if the rate of molecular formation is shorter than Δt , at most a fraction $\Delta t/t_{in}$ of injected atoms will be converted into molecules.

B. H₂ Formation in a Clean Grain

We consider the simplest case, namely molecular formation in a grain free of impurities ($n_{I\alpha} = \theta_{I\alpha} = 0$). We begin by giving explicit expressions for the rate coefficients in terms of the various parameters involved.

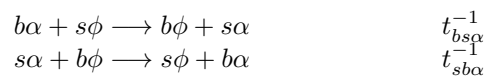
1. Reaction Rates

Below we list the processes included in the model. As a general strategy, we have parameterized the rates in terms of explicit functions of n_H , n_{H_2} , θ_H and θ_{H_2} (“fractional occupancies”) times characteristic rate coefficients (of the forms t^{-1} , αS). These latter depend primarily on T_g and various grain energy scales but also on occupancies when saturation is approached. (Later results are explicit and most useful when this implicit dependence on fractional occupancy is absent or weak but remain correct implicit solutions in all circumstances.)

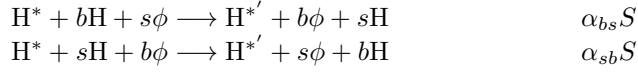
Let g_s and g_b be the fractions of all sites that are surface and bulk sites respectively (i.e. $\sim \mathcal{N}^{-1/3}$ and $1 - \mathcal{N}^{-1/3}$, up to a geometrical factor; $g_s + g_b = 1$). The fractional occupancies satisfy $0 \leq n_H + n_{H_2} \leq g_b$ and $0 \leq \theta_H + \theta_{H_2} \leq g_s$. We denote an empty bulk site $b\phi$; the probability that a bulk site is empty is $B^b = 1 - (n_H + n_{H_2})/g_b$. Likewise, we denote an empty surface site $s\phi$; the probability that a surface site is empty is $B^s = 1 - (\theta_H + \theta_{H_2})/g_s$.

The reactions are listed and the forms for the characteristic rate coefficient are given immediately to the right, followed by a short description of each process and the expression for the rate of change (always expressed as per site for the \mathcal{N} grain sites).

- Particle Exchange



- Thermally activated diffusion of a species $\alpha = \text{H}$ or H_2 from the bulk to the surface and vice versa. The fluxes are proportional to the product of bulk (surface) concentration and the number of vacant neighbor surface (bulk) sites. The rates per site may be expressed as $t_{bs\alpha}^{-1} n_\alpha (g_s B^s / g_b)$, and $t_{sb\alpha}^{-1} \theta_\alpha B^b$ where $t_{bs\alpha}$ and $t_{sb\alpha}$ are characteristic timescales to hop to nearest neighbor sites. The hopping timescales depend on the grain temperature, the characteristic binding energies and the form of the interaction. We assume exchanges between neighboring lattice sites; order unity range variations are accommodated in the definition of the characteristic timescale. Detailed balance implies $t_{sb\alpha}^{-1} = \exp\{(E^s[\alpha] - E^b[\alpha])/kT_g\} t_{bs\alpha}^{-1}$. If $E^b[\alpha] - E^s[\alpha] = 0$ then $t_{bs\alpha} = t_{sb\alpha} \sim t_{h\alpha}$.

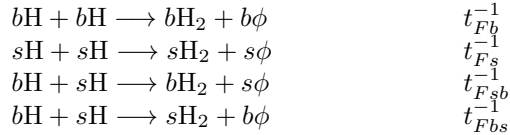


- Collisional displacement of H atoms from the bulk to the surface by energetic incident atoms (H^*) and vice versa. The rate coefficients are taken to be proportional to the total injection rate per site, $S = 1/\mathcal{N}t_{in}$, with efficiencies which are denoted by α_{bs} and α_{sb} , respectively. The rate per site for transport from bulk to surface takes the form $\alpha_{bs}S n_H (g_s B^s / g_b)$ and from surface to bulk, $\alpha_{sb}S \theta_H B^b$.

The efficiencies depend only on the energy of the incident particle and the energy level of the various sites as long as the density is smaller than the inverse volume sampled by the incident particle. Once the grain becomes saturated the efficiency of collisional displacement will depend on density, for example, when one dislodged atom can dislodge additional atoms.

A plausible limiting efficiency may be derived as follows. If in slowing down, an incident atom visited every site in the grain once, then each occupying atom suffers ~ 1 displacement. A surface atom is moved into the bulk with order unity probability; a bulk atom is moved into the surface with probability g_s . From the form of the above rate expressions, this corresponds to α_{bs} and $\alpha_{sb} \sim \mathcal{N}$. Thus, we assume that the efficiencies range from zero to roughly \mathcal{N} .

- H_2 formation and destruction



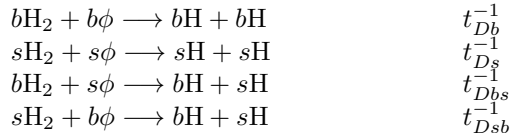
- Molecular hydrogen formation in the bulk and on the surface (reaction pathways labeled 1 and 2 in figure 2). We define t_{Fb} (t_{Fs}) to be the H_2 formation time, given that two H atoms are in neighboring, bulk (surface) sites. We define t_{Fbs} (t_{Fsb}) to be the time of H_2 formation on the surface (bulk) by recombination of subsurface and surface atoms. If H_2 formation in or on the grain is forbidden then $t_{Fi} = t_{Fij} = \infty$, while in the absence of an activation barrier $t_{Fb} \sim t_h$. Generally t_{Fi} are finite and depend on the height and width of the corresponding activation barriers for H_2 formation in the solid, as depicted in figure 2. The rate per site for H_2 formation in the bulk is $[t_{Fb}^{-1} n_H + t_{Fsb}^{-1} \theta_H] n_H / g_b$, and that for H_2 formation on the surface $[t_{Fs}^{-1} (\theta_H / g_s) + t_{Fbs}^{-1} (n_H / g_b)] \theta_H$. As above, we have assumed that the hydrogen pair interaction range is one lattice spacing but the variation may be absorbed into the definition of t_{Fi} .



- H_2 formation in the bulk by direct recombination of injected atoms with interstitial atoms. The rate of change of n_{H_2} is given by $\alpha_{Fb}S n_H$ where the efficiency α_{Fb} depends only on the energy of the incident atom and the site binding energy. Again, α_{Fb} ranges between zero and \mathcal{N} . If H_2 formation in the bulk is forbidden, then $\alpha_{Fb} = 0$.

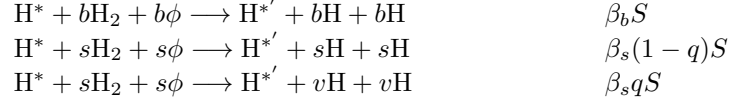


- H_2 formation on the surface by direct recombination with the incident atom. The corresponding rate of change of θ_{H_2} is given by $\alpha_{Fs}S\theta_H$ where the efficiency is α_{Fs} . A fraction δ_{Fs} of the formed molecules are assumed to remain on the surface, while the rest are immediately ejected from the grain. Following Duley⁴⁶, we shall refer to the latter process as prompt reaction.



- H_2 dissociation in or on the solid owing to thermal activation and quantum tunneling (in the case where metastable states exist). Detailed balance implies that the ratio of formation to dissociation rate $t_{Fi}^{-1}/t_{Di}^{-1} = \exp(2E_d^i/kT_g)$, $i = b, s$. We take the dissociation rate per site to be $t_{Db}^{-1} n_{\text{H}_2} B^b$ in the bulk, $t_{Ds}^{-1} \theta_{\text{H}_2} B^s$ on the surface. Likewise the rate coefficient for dissociation of H_2 in the bulk giving surface and subsurface H

is $t_{Dbs}^{-1} = t_{Fsb}^{-1} \exp\{-(2E_d^b + E[H]^s - E[H]^b)/kT_g\}$; for H_2 on the surface the corresponding rate coefficient is $t_{Dsb}^{-1} = t_{Fbs}^{-1} \exp\{-(2E_d^s + E[H]^b - E[H]^s)/kT_g\}$. The rates become $t_{Dbs}^{-1} n_{H_2} (g_s B^s / g_b)$ and $t_{Dsb}^{-1} \theta_{H_2} B^b$, respectively.



- H_2 dissociation in or on the solid by injected atoms. The bulk and surface dissociation rates per site are $\beta_b S n_{H_2} B^b$ and $\beta_s S \theta_{H_2} B^s$ where β_i gives the average number of dissociations per target molecule per site as the atom slows down for $i = b, s$. Further, we suppose that a fraction q of H_2 dissociations on the surface results in the immediate loss of the H atoms thereby produced from the grain.

- Particle Losses

- Thermal evaporation of H atoms from the grain's surface at a rate $\gamma_H \theta_H$.
- Collisional ejection of H atoms from the grain's surface at a rate $\alpha_{svH} S \theta_H$.
- Evaporation of H_2 molecules from the surface (thermal and quantum traversal of pathway 4 in figure 2) at a rate given by $\gamma_{H_2} \theta_{H_2}$.
- Collisional ejection of H_2 molecules from the grain's surface at a rate $\alpha_{svH_2} S \theta_{H_2}$.
- Pair recombination of adjacent surface atoms (thermal and quantum association via pathway 3 in figure 2), with a rate given by $g_s^{-1} \Gamma_{2H} \theta_H^2$. We henceforth refer to this process as “pair evaporation.”

For our models we need only the *sum* of various individual processes. These are:

- The rate coefficient for bulk to surface exchange is $\tau_{bsH}^{-1} = t_{bsH}^{-1} + \alpha_{bs} S$; the total rate is $n_H (g_s B^s / g_b) \tau_{bsH}^{-1}$. Likewise, the rate coefficient for surface to bulk exchange is $\tau_{sbH}^{-1} = t_{sbH}^{-1} + \alpha_{sb} S$; the total rate is $\theta_H B^b \tau_{sbH}^{-1}$. The rate coefficients for H_2 exchange are completely analogous.
- The dissociation rate coefficient on the surface is $\tau_{Ds}^{-1} = t_{Ds}^{-1} + \beta_s S$; in the bulk $\tau_{Db}^{-1} = t_{Db}^{-1} + \beta_b S$; and for surface plus subsurface products t_{Dbs}^{-1} and t_{Dsb}^{-1} . We also define the part of the surface dissociation rate that leads to an increase of θ_H (as opposed to immediate escape) $\tilde{\tau}_{Ds}^{-1} = \tau_{Ds}^{-1} - q \beta_s S$.
- The rate coefficient for thermal and collisional loss of H from the surface (all linear in θ_H) is $\Gamma_H = \gamma_H + \alpha_{svH} S$. The rate coefficient for H_2 loss by thermal, quantum and collisional loss is $\Gamma_{H_2} = \gamma_{H_2} + \alpha_{svH_2} S$.
- The H_2 formation rate in the bulk is $n_H (t_{Fb}^{-1} n_H / g_b + t_{Fsb}^{-1} \theta_H / g_b + \alpha_{Fb} S)$; the thermally driven H_2 formation rate on the surface is $\theta_H (t_{Fs}^{-1} \theta_H / g_s + t_{Fbs}^{-1} n_H / g_b)$; the H_2 formation rate by collisions and by pair evaporation is $\theta_H (\alpha_{Fs} S + g_s^{-1} \Gamma_{2H} \theta_H)$.

2. Relation of Rate Coefficients to Energy Scales

We now turn to the evaporation rates. We suppose that the interaction potential of a single hydrogen atom with the surface is similar to that shown schematically in figure 1, with $E_e > 0$. The evaporation rate of an H atom from a surface site is

$$\gamma_H = \nu_o \exp\{-E_e/kT_g\}, \quad (13)$$

where $\nu_o \sim 10^{13} \text{ s}^{-1}$ is the characteristic frequency of oscillation of an H atom about its equilibrium position.

The pair evaporation rate, Γ_{2H} , depends on the shape of the pair surface potential. Atom pairs can escape from the surface by either hopping above the finite activation barrier or if $E_c > 0$ by tunneling through it¹⁶. When $E_c > 0$ recombination can take place even at zero temperature and tunneling dominates the overbarrier rate at sufficiently low temperatures. In the following, we assume that the initial separation between the recombining atoms is of the order of the H-H interaction range (about 1 - 2 surface sites).

We consider first a grain with $E_c > 0$ at zero temperature, as shown in figure 1(i) and (iv). Let \mathbf{R} be the vector position of the center of mass of the pair system, \mathbf{r} one-half the relative position vector of the nuclei, and $V(\mathbf{r}, \mathbf{R})$ the

corresponding adiabatic potential. To zeroth order, the penetration factor of an atom pair of energy E along a given path joining the points a and b in this six-dimensional space, is given in the WKB approximation by

$$G_S = 2(2m_{2H}/\hbar^2)^{1/2} \int_a^b dS [V(\mathbf{r}(S), \mathbf{R}(S)) - E]^{1/2}, \quad (14)$$

where dS is a line element, and $V(a) = V(b) = E$. The transmission coefficient can be determined by summing e^{-G_S} over all paths joining the points a and b , and the corresponding tunneling rate is obtained by multiplying the result by ν_o , the attempt frequency. Lagrange's equations describe the path of minimum penetration factor for fixed endpoints a and b . The dominant contribution to the tunneling rate comes from that path and to a good approximation at zero temperature the surface recombination rate is

$$\Gamma_{2H} \simeq \nu_o e^{-G}, \quad (15)$$

where G denotes the appropriate value of G_S . To simplify the analysis further, we consider only paths along which \mathbf{r} is constrained to be parallel to the surface. We assume that the potential energy surfaces are co-planer for fixed separation so that the potential depends only on the two coordinates z and r , where z is the height above the surface (i.e., the component of \mathbf{R} normal to the surface) and $r = |\mathbf{r}|$ is one-half the distance between the hydrogen nuclei. Then the penetration problem reduces to tunneling through an effective one-dimensional potential $v(z) = [V(z) - E][1 + (dr/dz)^2]$ where (dr/dz) describes the appropriate path. In view of the uncertainties in the 2D potential energy surfaces, we approximate $v(z)$ by an inverted harmonic oscillator potential with barrier height ΔE and width z_o . Then

$$G_H = 48.5(\Delta E/eV)^{1/2}(z_o/\text{\AA}) \quad (16)$$

and eq. (15) gives the zero temperature recombination rate. The result is easily generalized to finite temperatures. Averaging the tunneling rate over the Boltzmann distribution while regarding the transmission coefficient as unity for $E > \Delta E$ yields

$$\Gamma_{2H} = \frac{\nu_o}{G_H - \Delta E/kT_g} \left[G_H e^{-\Delta E/kT_g} - (\Delta E/kT_g) e^{-G_H} \right]. \quad (17)$$

The rate is strongly enhanced when the temperature approaches the tunneling temperature, $T_t = \Delta E/kG_H \simeq 2.4 \times 10^2 (\Delta E/eV)^{1/2} (z_o/\text{\AA})^{-1}$ K, and approaches the classical limit above T_t .

For materials with $E_c > 0$, the pair evaporation rate is given by eq. (17) with $\Delta E = E_r$ (see figure 1[i,iv]), and G_H the penetration factor at energy E_c , i.e. the ground state energy of the trapped particles. The limiting behavior is

$$\Gamma_{2H} = \nu_o e^{-G_H \min\left(\frac{T_t}{T_g}, 1\right)} \quad \text{if } E_c > 0. \quad (18)$$

For materials $E_c < 0$, thermal activation is required (see figure 1[ii,iii]). Only atom pairs with total energy $\geq E[H_2]^v$ can tunnel through the barrier and we find that the surface recombination rate is eq. (17) reduced by a factor $\exp(-E_c/kT_g)$. Here, $\Delta E = E_a$ (see figure 1[ii,iii]) and the interpretation of G_H is that it is the penetration factor of an atom pair having energy $E[H_2]^v$. The limiting behavior is

$$\Gamma_{2H} = \nu_o e^{\frac{E_c}{kT_g}} e^{-G_H \min\left(\frac{T_t}{T_g}, 1\right)} \quad \text{if } E_c < 0. \quad (19)$$

In the case in which H_2 formation in or on the solid takes place, the evaporation of H_2 molecules from the grain surface proceeds in an analogous fashion. If $E[H_2]^s > E[H_2]^v$, as assumed for figure 2, then H_2 escapes by both overbarrier and underbarrier transitions. On the other hand, if $E[H_2]^s < E[H_2]^v$ then H_2 requires thermal activation to escape. Like Γ_{2H} , the H_2 evaporation rate, γ_{H_2} , depends on the energy barrier and whether or not tunneling can occur at zero temperature.

3. Rate Equations

We suppose that the occupation numbers are homogeneous in the bulk and (separately) on the surface. As already mentioned above, this assumption is justified when the diffusion time is short enough. The equations governing n_H , n_{H_2} , θ_{H_2} and θ_H are given respectively by,

$$\begin{aligned} \dot{n}_H = & S_H - [\tau_{bsH}^{-1}(g_s B^s/g_b) + 2\alpha_{Fb} S] n_H - 2g_b^{-1} t_{Fb}^{-1} n_H^2 + \tau_{sbH}^{-1} B^b \theta_H \\ & + (2\tau_{Db}^{-1} B^b + t_{Dbs}^{-1} g_s B^s/g_b) n_{H_2} + t_{Dsb}^{-1} B^b \theta_{H_2} - g_b^{-1} (t_{Fsb}^{-1} + t_{Fbs}^{-1}) n_H \theta_H, \end{aligned} \quad (20)$$

$$\begin{aligned} \dot{n}_{H_2} = & -[\tau_{Db}^{-1}B^b + (g_s B^s/g_b)t_{Dbs}^{-1} + \tau_{bsH_2}^{-1}(g_s B^s/g_b)]n_{H_2} + \alpha_{Fb}S n_H \\ & + t_{Fb}^{-1}g_b^{-1}n_H^2 + \tau_{sbH_2}^{-1}B^b\theta_{H_2} + g_b^{-1}t_{Fsb}^{-1}n_H\theta_H, \end{aligned} \quad (21)$$

$$\begin{aligned} \dot{\theta}_{H_2} = & \tau_{bsH_2}^{-1}n_{H_2}(g_s B^s/g_b) + t_{Fs}^{-1}g_s^{-1}\theta_H^2 + \alpha_{Fs}\delta_{Fs}S\theta_H + g_b^{-1}t_{Fbs}^{-1}n_H\theta_H \\ & - (\tau_{sbH_2}^{-1}B^b + \Gamma_{H_2} + \tau_{Ds}^{-1}B^s + t_{Dsb}^{-1}B^b)\theta_{H_2}, \end{aligned} \quad (22)$$

and

$$\begin{aligned} \dot{\theta}_H = & \mathcal{S}_H + \tau_{bsH}^{-1}n_H(g_s B^s/g_b) - (\tau_{sbH}^{-1}B^b + 2\alpha_{Fs}S + \Gamma_H)\theta_H - 2(\Gamma_{2H} + t_{Fs}^{-1})g_s^{-1}\theta_H^2 \\ & - (t_{Fsb}^{-1} + t_{Fbs}^{-1})g_b^{-1}n_H\theta_H + (2\tilde{\tau}_{Ds}^{-1}B^s + t_{Dsb}^{-1}B^b)\theta_{H_2} + (g_s B^s/g_b)t_{Dbs}^{-1}n_{H_2}. \end{aligned} \quad (23)$$

In steady state $\dot{n}_H = \dot{n}_{H_2} = \dot{\theta}_{H_2} = \dot{\theta}_H = 0$. Then the sum of eqs. (20) and (23) and twice eqs. (21) and (22) yields,

$$S = S_H + \mathcal{S}_H = t_{H-out}^{-1} + 2t_{H_2-out}^{-1}$$

where the loss rate of H to the vacuum is

$$t_{H-out}^{-1} = \Gamma_H\theta_H + 2B^s(\tau_{Ds}^{-1} - \tilde{\tau}_{Ds}^{-1})\theta_{H_2} = \Gamma_H\theta_H + 2q\beta_sSB^s\theta_{H_2},$$

and the loss rate of H_2 to the vacuum is

$$t_{H_2-out}^{-1} = \Gamma_{H_2}\theta_{H_2} + g_s^{-1}\Gamma_{2H}\theta_H^2 + \alpha_{Fs}S\theta_H(1 - \delta_{Fs}).$$

The efficiency of H_2 formation is the fraction of hydrogen released from the grain in molecular form:

$$\mathcal{E} = \frac{2t_{H_2-out}^{-1}}{t_{H-out}^{-1} + 2t_{H_2-out}^{-1}} = 1 - \frac{t_{H-out}^{-1}}{S}. \quad (24)$$

Let us examine the solution to the above equations in various limits. First, suppose that the timescales for H_2 formation and thermal dissociation on the surface, t_{Fs} and τ_{Ds} , are much shorter than any other timescale involved. We then anticipate the H and H_2 to be in equilibrium on the surface. Indeed, in the limit where all the rates except the formation and dissociation rates tend to zero, equations (22) and (23) yield, $B^s(\theta_{H_2}/g_s) = (\tau_{Ds}/t_{Fs})(\theta_H/g_s)^2 = e^{2E_d^s/kT_g}(\theta_H/g_s)^2$, which is just the appropriate mass action law (note E_d^s is the dissociation energy per atom). Similarly, when H_2 formation and dissociation are the dominant processes in the bulk, eqs. (20) and (21) yield, $(n_{H_2}/g_b)B^b = (\tau_{Db}/t_{Fb})(n_H/g_b)^2 = e^{2E_d^b/kT_g}(n_H/g_b)^2$. Next, suppose that the surface (bulk) to bulk (surface) diffusion times are very short compared with any other timescale. Upon taking the limit where all rates except the exchange rates tend to zero in eqs. (20) and (23), we recover the equilibrium distribution of H: $B^b(\theta_H/g_s) = B^s(t_{sbH}/t_{bsH})(n_H/g_b) = B^s \exp\{(E[H]^b - E[H]^s)/kT_g\}(n_H/g_b)$. Finally, in the limit where the H evaporation time is much shorter than quantum pair recombination, H_2 formation and dissociation on the surface, and transfer times from bulk to surface and vice versa, we obtain from eq. (23), $\theta_H = \mathcal{S}_H/\Gamma_H$, as expected. Likewise, when the pair recombination rate dominates, eq. (23) gives $\theta_H = (g_s\mathcal{S}_H/2\Gamma_{2H})^{1/2}$.

In the following, we shall neglect the densities in the statistical factors, as well as the surface-subsurface reactions. Specifically, we set $B^s = B^b = 1$, $t_{Fsb}^{-1} = t_{Fbs}^{-1} = t_{Dsb}^{-1} = t_{Dbs}^{-1} = 0$. This approximation enables us to solve eqs. (20) through (23) analytically in various regimes. The neglect of the densities in the statistical factors is certainly justified when the grain is unsaturated (i.e., $n_H + n_{H_2} \ll g_b$, $\theta_H + \theta_{H_2} \ll g_s$), a condition we check in our solutions. The full numerical solution of eqs. (20)-(23) indicates that this is a good approximation even for relatively large concentration numbers. In ignoring cross terms between the surface and bulk we are essentially assuming that the mixed rates are not larger than the corresponding rates in both the surface and the bulk. We have checked our results in a variety of limits and find no qualitative difference for the parameter ranges we have explored.

4. Equations without H_2 Formation/Destruction in the Bulk

We now explore the conditions required for effective H_2 formation in different regimes. First, consider a grain for which neither formation nor destruction of H_2 is possible in the bulk. This corresponds to the limit $\alpha_{Fb} = t_{Fb}^{-1} = t_{Db}^{-1} = \beta_b = 0$ in eqs. (20) - (23). Then eq. (20) can be written in the form,

$$n_H(a_1, a_2, a_3, a_4) = a_3\theta_H(a_1, a_2) + a_4, \quad (25)$$

eq. (21),

$$n_{H_2}(a_1, a_2, a_5, a_6, a_7) = a_7\theta_{H_2}(a_1, a_2, a_5, a_6), \quad (26)$$

and eq. (22),

$$\theta_{H_2}(a_1, a_2, a_5, a_6) = a_5\theta_H^2(a_1, a_2) + a_6\theta_H(a_1, a_2). \quad (27)$$

The sum of eqs.(20) and (23) gives the following dimensionless equation for the surface occupation probability:

$$1 - a_1\theta_H(a_1, a_2) - a_2\theta_H^2(a_1, a_2) = 0. \quad (28)$$

Here

$$\begin{aligned} a_1 &= \Gamma_H S^{-1} + 2\bar{\alpha}_{Fs}; & \bar{\alpha}_{Fs} &= \alpha_{Fs} \left(1 - \frac{\delta_{Fs}\tilde{\tau}_{Ds}^{-1}}{\tau_{Ds}^{-1} + \Gamma_{H_2}} \right), \\ a_2 &= 2g_s^{-1}S^{-1}(\Gamma_{2H} + \bar{t}_{Fs}^{-1}); & \bar{t}_{Fs}^{-1} &= t_{Fs}^{-1} \left(1 - \frac{\tilde{\tau}_{Ds}^{-1}}{\tau_{Ds}^{-1} + \Gamma_{H_2}} \right), \\ a_3 &= (g_b/g_s)(\tau_{bsH}/\tau_{sbH}), \\ a_4 &= (g_b/g_s)\tau_{bsH}S_H, \\ a_5 &= \frac{g_s^{-1}t_{Fs}^{-1}}{\tau_{Ds}^{-1} + \Gamma_{H_2}}, \\ a_6 &= \frac{\alpha_{Fs}\delta_{Fs}S}{\tau_{Ds}^{-1} + \Gamma_{H_2}}, \\ a_7 &= (g_b/g_s)(\tau_{bsH_2}/\tau_{sbH_2}), \end{aligned} \quad (29)$$

are dimensionless parameters that depend on the basic physical parameters as stated explicitly above.

As seen from eqs. (28) and (29), the surface occupation number, θ_H , depends on only two of the seven dimensionless parameters of the problem. For example, only the total injection rate (S) but not the individual bulk (S_H) and surface (S_H) injection rates are relevant for the value of θ_H . Since there is no interconversion of H and H_2 inside the grain, in steady state every atom intercepted by the grain must eventually escape through the surface. We will exploit the dependence of θ_H on a_1 and a_2 in the discussion in the next two sections. Note that in the simplest case with no H_2 formation on the surface ($t_{Fs}^{-1} = 0$), no prompt reaction ($\alpha_{Fs} = 0$) and pair evaporation only by quantum tunneling we have $-\ln a_1 \propto -\ln \Gamma_H \propto E_e/kT_g$ and $-\ln a_2 \propto -\ln \Gamma_{2H} \propto G_H$. The essential microphysical parameters that govern the surface H density are E_e and G_H . We will begin by characterizing the solutions to the steady-state problem directly in terms of possible combinations of E_e and G_H . We will then argue that more general cases are directly and simply described in terms of similar regions expressed as functions of $-\ln a_1$ and $-\ln a_2$, the analogues of E_e and G_H .

Although the surface density depends solely on a_1 and a_2 , all the dimensionless parameters are needed to find a full solution. That is important because we must check for saturation of surface and bulk components as well as calculate \mathcal{E} .

5. H_2 Formation by Pair Evaporation and/or Prompt Reaction

To elucidate the role of pair evaporation and prompt reaction, we further assume a grain for which H_2 is unstable on the surface. This corresponds to the limit $\tau_{Ds} \rightarrow 0$, $\tau_{Ds}/\tilde{\tau}_{Ds} \rightarrow 1$ in eq. (29). Then, $a_2 = 2g_s^{-1}\Gamma_{2H}/S$ and $a_5 = a_6 = 0$. Eqs. (26) and (27) then implies, $n_{H_2} = \theta_{H_2} = 0$. Now, when $a_4 > g_b$ the injection rate of H atoms into bulk sites, S_H , exceeds the rate at which hydrogen is released from the bulk, $g_s\tau_{bsH}^{-1}$, so the bulk will become saturated regardless of the values of the other parameters, as may be seen from eq. (25). If $a_4 \ll g_b$ bulk occupancy is controlled essentially by H transfer from the surface to the bulk rather than injection of H in the bulk, that is, by the first term rather than the second on the right hand side of eq. (25). The grain will remain unsaturated if the evaporation, surface recombination or prompt reaction rates are sufficiently large. (The efficiency $\mathcal{E} = 1 - \Gamma_H\theta_H/S$ (see eq. [24]) is also independent of a_4 .) Provided we are not interested in the exact value of n_H so long as it remains below g_b we can proceed by setting $a_4 = 0$ in eq. (25). The solution for n_H is then exact in situations in which

the ambient gas is cold, such that H atoms can only stick to the surface (i.e., $S_H = 0$, $\mathcal{S}_H = S$), and is a good approximation in general, provided that the rate at which H atoms are intercepted by the bulk is much smaller than the characteristic rate of transfer from the bulk to the surface.

When $a_3 < g_b/g_s$, or equivalently $\tau_{bsH}/\tau_{sbH} < 1$, the steady-state distribution of hydrogen in the grain always satisfies $n_H/g_b < \theta_H/g_s$. Consequently, when the surface reaches saturation the bulk remains unsaturated. When $a_3 > g_b/g_s$, bulk saturation always precedes surface saturation. Let us define a critical surface concentration above which the grain (either bulk or surface) is saturated:

$$\theta_{sat}/g_s = \begin{cases} 1; & \tau_{bsH}/\tau_{sbH} < 1 \text{ surface saturated} \\ \tau_{sbH}/\tau_{bsH}; & \tau_{bsH}/\tau_{sbH} > 1 \text{ bulk saturated.} \end{cases} \quad (30)$$

If thermal diffusion alone is responsible for surface-bulk fluxes, then $\tau_{bsH}/\tau_{sbH} = t_{bsH}/t_{sbH} = e^{-(E_s - E_c)/kT_g}$ and the top line applies for $E_s > E_c$, the bottom for $E_s < E_c$. The critical surface concentration has the simplest form ($\theta_{sat} = g_s$) when $E_s > E_c$. The condition for either bulk or surface to be saturated is temperature dependent when $E_s < E_c$ or whenever the rate coefficient includes collisionally driven exchange. At several points in this paper we will make the further assumption that the equations governing surface concentrations continue to apply even after the bulk has become saturated. Formally, the blocking factors that we have dropped would ensure mathematically well-defined solutions. The critical assumption is really that the basic grain parameters, measured or calculated for low occupancy continue to remain accurate in the saturated limit.

On substituting θ_{sat} into eq. (28), we obtain the equation of a surface in the space of physical parameters that separates the regimes of saturated and unsaturated grain. Specifically, the condition that the grain will be unsaturated reads,

$$\frac{\Gamma_{2H}}{\nu_o} > \left(\frac{g_s S}{2\theta_{sat}\nu_o} \right) \left(\theta_{sat}^{-1} - 2\bar{\alpha}_{Fs} - \frac{\Gamma_H}{S} \right) \quad (31)$$

with

$$\frac{\Gamma_H}{\nu_o} = \exp(-E_e/kT_g) + \frac{\alpha_{svH}S}{\nu_o} \quad (32)$$

where eq. (28) together with the definitions of the various physical parameters given above have been used. This inequality may be viewed as a relation between Γ_{2H} and E_e/kT_g when other parameters are fixed. In the absence of collisional ejections and prompt reactions the grain will be unsaturated either if $\Gamma_{2H} > g_s S / 2\theta_{sat}^2$ or if $E_e/kT_g < \ln(\nu_o \theta_{sat} / S)$.

In a similar manner, we can derive an equation describing a family of isoefficiency surfaces, where the efficiency is defined in eq. (24):

$$\frac{\Gamma_{2H}}{\nu_o} = \frac{g_s \Gamma_H}{2(1 - \mathcal{E})^2 S \nu_o} (\mathcal{E} \Gamma_H - 2(1 - \mathcal{E}) \bar{\alpha}_{Fs} S). \quad (33)$$

Note that the isosurfaces are independent of the timescales τ_{sbH} and τ_{bsH} (and θ_{sat}), as one might expect, since (i) evaporation and H₂ formation processes are restricted to the surface in the example presented here, and (ii) as already emphasized, the surface concentration depends on the total injection rate alone. In the absence of collisional ejections and prompt reactions eq. (33) assumes the simple form, $-\ln(\Gamma_{2H}/\nu_o) = 2E_e/kT_g + \ln[2S(1 - \mathcal{E})^2/(\mathcal{E}g_s\nu_o)]$.

Projections of the surfaces governed by eqs. (31) (when the inequality sign is replaced by the equal sign) and (33) onto the plane defined by $-\ln(\Gamma_{2H}/\nu_o)$ and E_e/kT_g are exhibited graphically in figure 3, for $g_s = 10^{-2}$, and different choices of the remaining parameters (note that the dependence of the curves on g_s as well as the other physical parameters besides $-\ln(\Gamma_{2H}/\nu_o)$ and E_e/kT_g is logarithmic). The regimes of saturated grain, effective and ineffective H₂ formation are indicated. The regions indicated as effective and ineffective in the figures are separated by the curves along which the efficiency $\mathcal{E} = 1/2$. In the regimes indicated as effective the pair evaporation rate exceeds the evaporation rate of H and in those indicated as ineffective the opposite is true. Windows (a) and (b) present a system not subject to direct collisional processes ($\alpha_{svH} = \alpha_{Fs} = 0$). The region enclosed by the solid line in case (a) corresponds to a saturated surface, whereas the regions enclosed by the curves labeled by values of $\tau_{bsH}/\tau_{sbH} > 1$ correspond to bulk saturation. Note that for any given substance, θ_{sat} is variable, as discussed above. (In a later section we speculate upon the steady state of grains saturated with hydrogen, and discuss several plausible scenarios for H₂ formation in such systems.)

It should be noted that Γ_{2H} is constant only in the limit of zero temperature quantum tunneling. The pair evaporation rate generally depends on the grain temperature and $\Gamma_{2H} \rightarrow \nu_o$ as $T_g \rightarrow \infty$. For $E_c > 0$, the limiting form

for pair recombination (eq. [18]) implies $-\ln(\Gamma_{2H}/\nu_o) \simeq (E_r/E_e)(E_e/kT_g)$ at grain temperatures above the tunneling temperature T_t , and $-\ln(\Gamma_{2H}/\nu_o) \simeq G_H$ below; for $E_c < 0$ the limiting form (eq. [19]) implies $-\ln(\Gamma_{2H}/\nu_o) \simeq [(E_a - E_c)/E_e](E_e/kT_g)$ above, and $-\ln(\Gamma_{2H}/\nu_o) \simeq G_H - E_c/kT_g$ below. In figure 4, we show the dependence of pair evaporation rate on grain temperature ($-\ln\Gamma_{2H}/\nu_o$ is plotted against E_e/kT_g) for two materials. The dashed line describes a typical transition metal with $E_e = 2.55$ eV, $E_c = -0.3$ eV, $E_a = 0.2$ eV, and $G_H > 7$. The dotted-dashed line describes carbon (with $E_c > 0$) using the same parameters adopted in §V, namely $E_e = 0.3$ eV, $E_r = 0.4$ eV, and $G_H = 30$. The solid lines for efficiency and surface saturation were computed using the same parameters as in figure 3(a) with $\tau_{bsH}/\tau_{sbH} < 1$. Note that the conditions for bulk saturation are not displayed in this figure. In the case of carbon we find that bulk saturation occurs (for $E_s = -0.2$ eV, $S \simeq 10^{-13}$ s $^{-1}$, and the above choice of the remaining parameters, see §V for a detailed discussion) when $E_e/kT_g > 7$. For both of these putative materials the surfaces remain unsaturated. The threshold temperature below which effective H₂ formation takes place is $\sim 10^3$ K for the transition metal and ~ 90 K for carbon.

The effect of collisional ejection of H from the surface and prompt reaction is illustrated in figure 3 windows (c) and (d). The range of values of α_{svH} and $\bar{\alpha}_{Fs}$ shown in these windows encompasses most of the physically allowed range, namely from zero to \mathcal{N} (in which case every incident atom induces a reaction). In both cases the region labeled saturated shrinks with increasing values of the efficiencies α_{svH} and $\bar{\alpha}_{Fs}$, and eventually disappears when $\alpha_{svH} + 2\bar{\alpha}_{Fs} = \theta_{sat}^{-1}$ (see eq. [31]). The reason is that both processes involve release of hydrogen from the grain and, consequently, when $\alpha_{svH} + 2\bar{\alpha}_{Fs} = \theta_{sat}^{-1}$ the grain can be sustained unsaturated irrespective of the thermal and quantum release rates. For example, the dotted and dash-dotted curves in windows (c) and (d) correspond to a case where the grain is unsaturated in the entire $(-\ln\Gamma_{2H}/\nu_o, E_e/kT_g)$ plane. The panels show that the H₂ formation efficiency decreases with increasing α_{svH} and increases with increasing α_{Fs} . Because case (c) involves release of H atoms by direct collisions, the efficiency curves become independent of E_e for values larger than that at which the collisional ejection rate exceeds the thermal evaporation rate, that is, $\Gamma_H < \alpha_{svH}S$. Likewise, case (d) involves collisional formation followed by ejection of H₂ molecules and, therefore, the efficiency curves become independent of Γ_{2H}/ν_o for values such that $\Gamma_{2H} < \alpha_{Fs}S$.

6. H₂ from Surface Formation plus Pair Evaporation and Prompt Reaction

We now generalize the above analysis to grains whose surfaces can form and dissociate H₂ while continuing to assume no H₂ formation/dissociation in the bulk. Consequently, the rate constants τ_{Ds}^{-1} , t_{Fs}^{-1} and \bar{t}_{Fs}^{-1} assume non-trivial values and the definition of $\bar{\alpha}_{Fs}$ is modified. The dimensionless coefficients a_5 and a_6 acquire non-zero values but the previous analysis remains basically unchanged. In particular, the rate coefficients a_3 and a_4 and the expression for θ_{sat} remain unaltered. H saturation in the bulk still occurs when $a_4 > g_b$ irrespective of the values of the other parameters. The presence of H₂ formation on the surface does not change the characteristic release rate of H from the bulk. (This would not be true in the presence of H₂ formation in the bulk, because then hydrogen can be released from the bulk also in molecular form.) We proceed, as before, by setting $a_4 = 0$. For $q = 0$, (no ejections of H atoms following collisional dissociation on the surface) eq. (31), which gives the condition for H not being saturated, and eq. (33), which gives the efficiency, are modified as follows:

$$\Gamma_{2H} \rightarrow \Gamma_{2H} + \bar{t}_{Fs}^{-1} \quad (34)$$

$$= \Gamma_{2H} + \frac{t_{Fs}^{-1}\Gamma_{H_2}}{\tau_{Ds}^{-1} + \Gamma_{H_2}} \quad (35)$$

Since the rates of surface formation and pair evaporation are each quadratic in θ_H , the previous analysis is only altered by the change in the effective H₂ formation rate coefficient. The indicated change above clearly shows that the efficiency will increase when H₂ can form on the surface but the increase is qualitatively important only when pair evaporation and prompt reactions are ineffective by themselves ($S(\Gamma_{2H}/g_s\Gamma_H^2 + 2\alpha_{Fs}/\Gamma_H) \ll 1$) while the additional process is sufficiently rapid ($S\bar{t}_{Fs}^{-1}/g_s\Gamma_H^2 \gtrsim 1$). The form of \bar{t}_{Fs}^{-1} depends on the ratio of surface dissociation rate to evaporation rate for H₂. If evaporation is more rapid then $\bar{t}_{Fs}^{-1} \rightarrow t_{Fs}^{-1}$ and nearly every surface-formed H₂ escapes as soon as it is created. Efficient molecule formation requires $S\bar{t}_{Fs}^{-1}/g_s\Gamma_H^2 \gtrsim 1$. On the other hand, if dissociation is more rapid then H and H₂ obey a Saha-like equilibrium on the surface and the molecule escape rate is the evaporation rate of the H₂ fraction. Efficient formation requires $S\Gamma_{H_2}e^{2E_d^s/kT_g}/g_s\Gamma_H^2 \gtrsim 1$.

The formation of H₂ on the surface provides a source of molecular hydrogen on and in the grain and one must worry about the possibility of H₂ saturation in addition to H saturation. The region in the space spanned by the parameters a_1 through a_7 in which the grain is unsaturated by any component is determined, in terms of the solution of eqs. (25)-(28), by the set of inequalities,

$$\begin{aligned} \theta_H(a_1, a_2) + \theta_{H_2}(a_1, a_2, a_5, a_6) &< g_s \\ n_H(a_1, a_2, a_3, a_4) + n_{H_2}(a_1, a_2, a_5, a_6, a_7) &< g_b. \end{aligned} \quad (36)$$

This also defines the regime of unsaturated grain in the space of physical parameters through the dependence of a_1 - a_7 on them.

Rather surprisingly, it is possible to give an approximate compact analytic treatment of the above conditions. We have the limiting solutions for θ_H

$$\theta_H = \begin{cases} 1/a_1 & \text{for } a_1^2 \gg 4a_2 \\ 1/a_2^{1/2} & \text{for } a_1^2 \ll 4a_2 \end{cases} \quad (37)$$

and the condition that the grain (both surface and bulk) be unsaturated is

$$\theta_H^2 \ll \min \left(\frac{g_s}{a_5}, \left(\frac{g_s}{1+a_6} \right)^2, \frac{g_b - a_4}{a_5 a_7}, \left(\frac{g_b - a_4}{a_3 + a_6 a_7} \right)^2 \right) \quad (38)$$

Terms involving g_s (g_b) are the surface (bulk) constraints. (As discussed previously, if $g_b < a_4$ the bulk must become saturated.) These inequalities guarantee that the regions of saturated and unsaturated grains will be identical in shape to those shown in window (a) of figure 3 in which the axes are relabeled, viz.

$$\begin{aligned} \frac{E_e}{kT_g} &\rightarrow -\ln \frac{S a_1}{\nu_o} \\ \Gamma_{2H} &\rightarrow \frac{g_s S a_2}{2} \end{aligned} \quad (39)$$

and the numerical values for the horizontal and vertical lines are determined from the above list.

It is also straightforward to show that the limiting forms for efficiency for $q = 0$ are

$$\mathcal{E} = \begin{cases} \left(\frac{2\alpha_{Fs} S}{\Gamma_H + 2\alpha_{Fs} S} \right) & \text{for } a_1^2 \gg 4a_2 \\ 1 - \left(\frac{g_s \Gamma_H^2}{2S(\Gamma_{2H} + t_{Fs}^{-1})} \right)^{1/2} & \text{for } a_1^2 \ll 4a_2 \end{cases} \quad (40)$$

When $q \neq 0$, the efficiency is lowered by the amount $2q\beta_s\theta_{H_2}$.

7. H_2 Formation in the Bulk

Next, we wish to examine the conditions under which effective H_2 formation may take place in the bulk, and explore the different regimes in parameter space in which grain saturation by H and/or H_2 occurs. Since the inclusion of quantum pair evaporation complicates the analysis considerably, and can only lead to a higher H_2 formation efficiency anyway, we ignore it in the present example. We also ignore H_2 formation and dissociation on the surface (but keep the prompt reaction process) in order to simplify the analysis further. The complementary case in which H_2 formation is controlled entirely by the surface has been studied in the previous example.

Consider a grain for which H_2 formation in the bulk is allowed but H_2 formation and destruction on the surface as well as quantum pair evaporation are negligible. We set $t_{Fs}^{-1} = \delta_{Fs} = \tau_{Ds}^{-1} = \Gamma_{2H} = 0$ in eqs. (20)-(23). One then finds,

$$1 - b_1 n_H - b_2 n_H^2 = 0, \quad (41)$$

with

$$\begin{aligned} b_1 &= \left(\frac{2\alpha_{Fb}}{1+\eta} + \left(\frac{g_s \tau_{sbH}}{g_b \tau_{bsH}} \right) \frac{\Gamma_H/S + 2\alpha_{Fs}}{1 + \tau_{sbH}(\Gamma_H + 2\alpha_{Fs}S)} \right) r \\ b_2 &= \frac{2}{g_b t_{Fb} S (1+\eta)} r \end{aligned} \quad (42)$$

and we have introduced two auxiliary variables to simplify the notation:

$$\eta = \frac{g_b(1 + \tau_{sbH_2}\Gamma_{H_2})\tau_{bsH_2}}{g_s\tau_{sbH_2}\Gamma_{H_2}\tau_{Db}}$$

$$\frac{1}{r} = \frac{S_H}{S} + \frac{S_H}{S(1 + \tau_{sbH}(\Gamma_H + 2\alpha_{Fs}S))}. \quad (43)$$

It can be easily verified that in the absence of H_2 formation inside the grain, which corresponds to the limit $t_{Fb}^{-1} = \alpha_{Fb} = 0$, the solution of eq. (41), given by $n_H = 1/b_1$, coincides with the solution of eq. (25) and (28) for $\Gamma_{2H} = 0, \tau_{Ds} = 0$ as required. Note that the quadratic coefficient $b_2 \neq 0$ only if H_2 can form by thermal processes within the bulk and its effect is to lower n_H . The complexity of the linear coefficient b_1 arises from all the linear processes that alter the distribution of H (and H_2) in and on the grain including evaporation from the surface (Γ_H, Γ_{H_2}), transfer between bulk and surface ($\tau_{sbH}, \tau_{bsH}, \tau_{sbH_2}, \tau_{bsH_2}$), and collisional H_2 formation by particles incident on the bulk and on the surface (α_{Fb}, α_{Fs}).

The quantity $1/r$ is the equilibrium fraction of the incident H atoms available to the bulk. r lies in the range between 1, for $S_H \simeq S$ (as in the case of homogeneous injection for which $S_H = g_s S$ and $S_H = g_b S \simeq S$, provided that the grain is large enough), and $1 + \tau_{sbH}(\Gamma_H + 2\alpha_{Fs}S)$ for $S_H = 0$ (which corresponds to a situation where the ambient gas is cold such that atoms impinging on the grain stick to the surface and diffuse into the bulk). In the latter case, n_H approaches zero when the surface to bulk exchange time τ_{sbH} becomes much longer than the evaporation and prompt reaction timescales since the only source of bulk atomic hydrogen is the flux from the surface.

The coefficient η is the ratio of dissociation rate and net release rate of molecular hydrogen in the bulk. If τ_{Db} is much longer than the H_2 release time, viz., $\eta \ll 1$, almost every newly formed molecule will escape from the bulk before it dissociates and, consequently, the loss rate of bulk atomic hydrogen will depend on the molecule formation rate (thermally activated and collisional) alone. When $\eta \gg 1$, only a fraction η^{-1} of the newly formed molecules leave the bulk before they dissociate, so the loss rate of H in the bulk is reduced by a factor η^{-1} .

The surface occupation probability of H satisfies the equation,

$$\theta_H = b_3 n_H + b_4, \quad (44)$$

where eqs. (22) and (23) have been employed, and where

$$b_3 = \frac{g_s(\tau_{sbH}/\tau_{bsH})}{g_b[1 + \tau_{sbH}(\Gamma_H + 2\alpha_{Fs}S)]},$$

$$b_4 = \frac{\tau_{sbH}S_H}{1 + \tau_{sbH}(\Gamma_H + 2\alpha_{Fs}S)}. \quad (45)$$

The parameter b_3 represents the net contribution from the bulk to surface by exchange, whereas b_4 represents the contribution from direct injection of H atoms on the surface. When $\tau_{sbH}(\Gamma_H + 2\alpha_{Fs}S) \gg 1$, the loss of hydrogen atoms from the surface is dominated by prompt reaction, evaporation and direct ejections rather than transfer to the bulk. Then $(\Gamma_H + 2\alpha_{Fs}S)\theta_H \simeq g_s\tau_{bsH}^{-1}(n_H/g_b) + S_H$; that is, the loss of surface H atoms by evaporation, direct ejection, and prompt reaction is balanced by injection into surface sites plus transfer of H atoms from the bulk. In the opposite limit, $(\theta_H/g_s) \simeq (\tau_{sbH}/\tau_{bsH})(n_H/g_b) + \tau_{sbH}S_H/g_s$, which for sufficiently small surface injection rate ($\tau_{sbH}S_H \simeq 0$) approaches the equilibrium distribution (see discussion following eq. [23]).

The bulk and surface concentrations of molecular hydrogen depend on three additional parameters:

$$b_5 = \frac{\tau_{Db}}{g_b t_{Fb}} \left(\frac{\eta}{1 + \eta} \right),$$

$$b_6 = \alpha_{Fb} S \tau_{Db} \left(\frac{\eta}{1 + \eta} \right),$$

$$b_7 = \frac{1}{\eta \tau_{Db} \Gamma_{H_2}}. \quad (46)$$

In terms of these parameters, the solution for n_{H_2} takes the simple form

$$n_{H_2} = b_5 n_H^2 + b_6 n_H, \quad (47)$$

and that for θ_{H_2} ,

$$\theta_{H_2} = b_7 n_{H_2}. \quad (48)$$

The last equation reflects the fact that the only source of H₂ molecules on the surface is the flux of H₂ from the bulk. This is due to our neglect of H₂ formation on the surface.

In general, the regime of validity of the solution presented above is defined by:

$$\begin{aligned} n_H(b_1, b_2) + n_{H_2}(b_1, b_2, b_5, b_6) &< g_b, \\ \theta_H(b_1, b_2, b_3, b_4) + \theta_{H_2}(b_1, b_2, b_5, b_6, b_7) &< g_s. \end{aligned} \quad (49)$$

We now note that the substitution $b_i \rightarrow a_i$, the interchanges $n \leftrightarrow \theta$ and $g_b \leftrightarrow g_s$ yield exactly the same set of equations analyzed in the preceding section. Thus, we have the limiting solution n_H

$$n_H = \begin{cases} 1/b_1 & \text{for } b_1^2 \gg 4b_2 \\ 1/b_2^{1/2} & \text{for } b_1^2 \ll 4b_2 \end{cases} \quad (50)$$

and the condition that the grain (both surface and bulk) be unsaturated is

$$n_H^2 \ll \min \left(\frac{g_b}{b_5}, \left(\frac{g_b}{1+b_6} \right)^2, \frac{g_s - b_4}{b_5 b_7}, \left(\frac{g_s - b_4}{b_3 + b_6 b_7} \right)^2 \right) \quad (51)$$

When $b_4 > g_s$, the injection rate of hydrogen on the surface exceeds the rate at which H atoms are lost from the surface by evaporation, prompt reaction, and transfer to the bulk, as can be seen from eq. (45), and, therefore, surface saturation will occur regardless of the value of n_H .

In contrast to the problem of H₂ formation studied in the previous section, there is no simple relationship between b_1 and b_2 and the fundamental microphysical parameters (e.g. E_e/kT_g and G_H). This is already apparent in the original expressions for b_1 and b_2 which involve complex relationships between all the formation and release processes for H and H₂. Nonetheless, the above inequalities faithfully convey the conditions for surface and bulk to remain unsaturated.

We define the efficiency of H₂ formation as in the previous example: $\mathcal{E} = 1 - \Gamma_H \theta_H / S$. By employing eqs. (41) and (44), we can express \mathcal{E} as

$$\mathcal{E} = 1 - \Gamma_H S^{-1} [b_3 n_H(b_1, b_2) + b_4] = 1 - \Gamma_H S^{-1} \left\{ \frac{b_3}{2b_2} \left[-b_1 + \sqrt{b_1^2 + 4b_2} \right] + b_4 \right\}. \quad (52)$$

The efficiency is independent of the parameters b_5 through b_7 , as it measures only the ratio of escape rate (thermal evaporation plus direct ejections) to interception rate by the grain of H nuclei. It does not tell us anything about the values of bulk and surface concentrations of molecular hydrogen. The latter are determined by the rate coefficients b_5 , b_6 and b_7 , which involve ratios of H₂ formation rates to dissociation, release, and bulk to surface exchange rates, as seen from eq. (46).

To elucidate the solution further we consider the limit $\alpha_{F_s} = 0$ and $\mathcal{S}_H = 0$ ($r = 1$). The latter approximation implies $b_4 = 0$. We define

$$\begin{aligned} x_F &= 1/t_{Fb} S, \\ x_R &= \frac{g_s (\tau_{sbH} / \tau_{bsH}) (\Gamma_H / S)}{g_b (1 + \tau_{sbH} \Gamma_H)}. \end{aligned} \quad (53)$$

x_F is the thermally activated H₂ formation rate in the bulk in units of the injection rate per site, S . x_R is the net release rate per bulk H atom of atomic hydrogen from the bulk measured in units of S . For $\tau_{sbH} \Gamma_H \gg 1$, $x_R \simeq (g_s/g_b)(\tau_{bsH} S)^{-1}$, in which case H release from the bulk is limited by the rate at which H is transferred to the surface. For $\tau_{sbH} \Gamma_H \ll 1$, $x_R \simeq (g_s/g_b)(\tau_{sbH}/\tau_{bsH})(\Gamma_H/S)$ and the net release of H is limited by evaporation from the grain ($g_s \tau_{sbH}/g_b \tau_{bsH}$ is the equilibrium ratio of surface and bulk H concentrations).

Eq. (41) may be recast as a relation between the formation rate and the release rate for fixed n_H

$$x_R = \left(n_H^{-1} - \frac{2\alpha_{Fb}}{1+\eta} \right) - \frac{2n_H}{g_b(1+\eta)} x_F. \quad (54)$$

Likewise eq. (52) may be used to find contours of fixed efficiency in the (x_R, x_F) plane

$$x_F = \frac{g_b [\mathcal{E}(1+\eta)x_R^2 - 2(1-\mathcal{E})\alpha_{Fb}x_R]}{2(1-\mathcal{E})^2}. \quad (55)$$

Finally, once $b_4, b_5, b_6,$ and b_7 are fixed, the critical value of n_H for which the grain becomes saturated in or on can be computed from eq. (49).

Contours of n_H in the (x_R, x_F) plane are exhibited graphically in figure 5 (values of n_H label the curves), for $\alpha_{Fb} = 0, \eta = 0$ (solid lines) and $\eta = 10^2$ (dotted lines). When the release rate is large, then n_H is small (near the top). When the rate is small and the formation rate is small, then n_H is large (bottom right); while if the formation rate is large, then it is small (bottom left). Another way to view the results is as follows. The vertical portion of the curve (independent of x_R) corresponds to the regime where n_H is limited by H_2 formation; the horizontal portion (independent of x_F) is the regime where n_H is limited by release from the bulk. As η increases the curves move leftward. The reason, as already explained above, is that for $\eta > 1$ the rate at which hydrogen leaves the bulk in molecular form diminishes by η^{-1} and, therefore, shorter formation time (i.e., larger x_F) is required to maintain n_H at the same value, as also clearly seen from eq. (54). Also shown schematically in figure 5 is the curve separating the regimes of saturated and unsaturated grain (dashed line). The location of this curve depends on the values of the remaining parameters ($b_4 - b_7$) through eq. (49). The corresponding critical value of n_H can range between zero for $b_4 \geq g_s$ and $\sim g_b$.

The quantitative range of n_H is easily derived: For a given injection rate, n_H cannot exceed $n_o = (1 + \eta)/2\alpha_{Fb}$, when capture of H atoms in the bulk is balanced by release of H_2 molecules produced by direct collisions. For this value eq. (54) yields $x_R = 0, x_F = 0$. Sustaining n_H at values smaller than n_o requires, in addition to collisional formation of H_2 molecules, either thermally activated H_2 formation ($x_F > 0$), or H release ($x_R > 0$). For $n_H \ll n_o$ the latter processes dominate over collisional H_2 formation which ultimately becomes negligible.

Labeled efficiency contours are presented in figure 6 for $\eta = 0, \alpha_{Fb} = 0$ (solid lines) and $\alpha_{Fb} = 10^4$ (dashed lines). As seen, for large x_R (large release rate) the efficiency curves are power laws with slope 2, reflecting the dominance of thermally activated over collisional H_2 formation. As x_R approaches $2(1 - \mathcal{E})\alpha_{Fb}/\mathcal{E}$, the desired efficiency can be achieved by collisional H_2 formation alone and, hence, $x_F \rightarrow 0$.

8. Saturated Grain

What happens when the grain becomes saturated by either atoms or molecules? Presumably, the saturation of the grain affects the embedding energies and diffusion times considerably. Unfortunately, the dependence of those parameters on filling factors is poorly understood. Nevertheless, we can still draw some general conclusions. Consider a clean grain having a temperature T_g , initially devoid of H atoms and H_2 molecules, embedded in a gas of hydrogen atoms. Suppose first that molecular hydrogen formation in and on the grain is energetically unfavorable and/or inefficient (i.e., $t_{Fi} \rightarrow \infty$) and that the mean evaporation time of an H atom, the prompt-reaction time and the mean surface recombination time are all much longer than t_{in} . Then after a time $\sim \mathcal{N}t_{in}$ the grain will become saturated by H atoms. The evolution of the system from this point on will depend on the modified parameters. If the embedding energy of H atoms is not altered significantly, then a newly incident atom will either eject bound H atoms from the grain as a result of collisions provided that its energy is sufficiently large, push bulk atoms to the surface, or will stop inside the grain and then diffuse to the surface and stick. If the yield for the first process is much smaller than unity, then layers of atomic hydrogen should form on top of the original grain surface. Our expectation is that this will lead to a dramatic increase of the surface recombination rate and, consequently, effective H_2 formation, since the atom-surface binding energy declines sharply with distance from the original grain surface.

Next, consider the possibility that molecular hydrogen formation in or on the grain is effective, and that the mean evaporation time of a molecule is much longer than $2t_{in}$. The grain will become saturated by H_2 molecules after a time $\sim 2\mathcal{N}t_{in}$. A newly injected atom will then either break up a bound H_2 , ejecting one of the H atoms from the grain in the process, or be pushed from the bulk to the surface and then evaporate or stick, depending on the modified surface binding energy. If it sticks to the surface for a time longer than about t_{in} , it will eventually recombine with a second injected atom to form a molecule (under astrophysical conditions, the surface migration time is anticipated to be much shorter than t_{in}). This will lead to the growth of layers of molecular hydrogen until the evaporation rate of atoms or molecules exceeds the value required for steady-state.

Alternatively, it could be that when the filling factor becomes sufficiently large, a few per cent say, the embedding energies of H and H_2 are sufficiently reduced to allow the evaporation rate of either atoms or molecules to balance the flux of incident particles. The efficiency of molecular formation in this scenario would depend on the value of the modified parameters at steady-state. Our analysis should be applicable provided that the hydrogen has not undergone a phase transition to some ordered phase at these densities.

V. APPLICATION: H₂ FORMATION IN CARBON

As an example we consider H₂ formation in and on carbon grains. For simplicity, we take the distribution of H atoms in the gas phase to be isotropic and monoenergetic with respect to the grain, and denote by $n(\text{H})$ and ϵ the number density and energy (measured in units of eV) of the H atoms. The velocity of an H atom relative to the grain is then $v = 1.4 \times 10^6 (\epsilon/\text{eV})^{1/2} \text{ cm s}^{-1}$, and the flux impinging on the grain is $n(\text{H})v \simeq 4 \times 10^5 (\epsilon/\text{eV})^{1/2} n(\text{H}) \text{ cm}^{-2} \text{ s}^{-1}$. In terms of the transmission coefficient $T(\epsilon)$, defined in the text preceding eq. (1), and the characteristic grain size $a = a_{-5} 10^{-5} \text{ cm}$, we can approximate the injection rate as

$$t_{in}^{-1} \simeq 3 \times 10^{-4} n(\text{H}) (\epsilon/\text{eV})^{1/2} a_{-5}^2 T(\epsilon) \text{ s}^{-1}, \quad (56)$$

where the grain's geometrical cross section has been taken to be of order $4\pi a^2$ (ignoring possible focusing effects). Let d_{-8} be the average interatomic separation of C atoms in Å. Then the total number of sites is roughly $\mathcal{N} \simeq 4 \times 10^9 (a_{-5}/d_{-8})^3$ and the relative number of surface sites is of order $g_s \simeq 2 \times 10^{-3} (a_{-5}/d_{-8})^{-1}$. Thus,

$$S = (\mathcal{N} t_{in})^{-1} \simeq 7.5 \times 10^{-14} n(\text{H}) (\epsilon/\text{eV})^{1/2} a_{-5}^{-1} d_{-8}^3 T(\epsilon) \text{ s}^{-1}. \quad (57)$$

Hydrogen adsorption on carbon takes place in different types of sites with different activation energies. The experimental values of the activation energies for adsorption lie between about 0.3 and 2.2 eV^{44,47}. The heat of adsorption (or equivalently the embedding energy E_e , see §III D and figure 1) has not been determined experimentally yet. However, several attempts have been made to calculate it for the hydrogen graphite system using quantum chemical codes^{48,49}. The results of such calculations are highly uncertain, but seem to suggest the following: i) the most favorable site for chemisorption is the one which corresponds to the H atom being directly above a C atom. The embedding energy lies in the range between ~ 0.3 and 1.14 eV, implying E_c between 1.94 and 1.1 eV. ii) the activation energy for H pair recombination (E_r in figure 1) is about 0.4 eV. As mentioned in §III D, the detection of highly excited H₂ molecules formed on carbon surfaces at low temperatures led Schermann et al.³¹ to conclude that the embedding energy should not exceed ~ 0.3 eV, consistent with the results of ref.⁴⁹. For E_e in the range 0.3 – 1.1 eV and $E_r = 0.4$ eV, we obtain an activation energy of chemisorption in the range between 2.34 (note that this implies that there should be an activation barrier of ~ 0.1 eV for adsorption of atomic hydrogen) and 1.5 eV, respectively, consistent with the experimental values mentioned above.

Taking $E_r = 0.4$ eV, eq. (16) yields for the penetration factor at zero temperature $G_H \simeq 30(z_o/\text{Å})$, and eq. (17) gives $T_t \simeq 150(z_o/\text{Å})$ K for the tunneling temperature, where z_o is again the width of the barrier. In the absence of collisional processes eq. (31) with $\theta_{sat} = g_s$ implies that the surface will be maintained unsaturated at $T_g = 0$ provided that

$$\ln[n(\text{H})(\epsilon/\text{eV})^{1/2} d_{-8}^2 T(\epsilon)] < 54 - 30(z_o/\text{Å}). \quad (58)$$

As indicated above, we are ignoring the possibility that bulk saturation alters fundamental grain parameters and assume this condition to suffice even if the bulk is saturated. (We show that bulk saturation is likely below.) Adopting $z_o = 1\text{Å}$, $d = 3\text{Å}$, $T(\epsilon) \simeq 1$ for illustration, we find that quantum pair evaporation will keep the surface unsaturated as long as $n(\text{H})(\epsilon/\text{eV})^{1/2} < 2.5 \times 10^9 \text{ cm}^{-3}$. Increasing the grain temperature will result of course in a smaller surface concentration. Note that the condition (58) is independent of the grain size since both the incoming flux of H atoms and the outgoing flux of H pairs are proportional to the surface area.

If molecules form *only* by pair evaporation from the surface, the efficiency is given by eq. (33). Setting the collisional rates to zero and taking $\mathcal{E} = 1/2$ in eq. (33), we find that for the same choice of z_o , d and $T(\epsilon)$, the efficiency will exceed 1/2 if

$$T_g < T_{crt} = \frac{10^4 (E_e/1\text{eV})}{40 - \ln(n(\text{H})(\epsilon/\text{eV})^{1/2})/2} \text{ K}. \quad (59)$$

For example, for the value of E_e inferred by Schermann et al., viz., $E_e = 0.3$ eV, the last equation gives T_{crt} between about 75 and 100 K for $n(\text{H})(\epsilon/\text{eV})^{1/2}$ between 1 and 10^7 cm^{-3} , respectively. It is important to note that the efficiency \mathcal{E} defined in eq. (24) is essentially the probability that an H atom intercepted by the grain will be released as part of a molecule. The overall H₂ formation efficiency is the product of \mathcal{E} and the transmission (sticking or penetrating) probability of H.

If collisional displacement of H from bulk to surface does not occur and if molecule formation in the bulk does not occur then we find that the bulk will be saturated by H in steady state. Our reasoning follows. The solubility and diffusivity of hydrogen in the bulk are uncertain. The reported values of the diffusion energy range between 0.5 and 4.3 eV^{32,44}. This is most likely due to the broad spectrum of binding sites. The deepest sites are the trapping sites

thought to be associated with unsaturated carbon atoms on the edges of microcrystals constituting the amorphous material^{44,49}. The trap energy is of order 4.3 eV, comparable with the bond energy between H and C in typical hydrocarbons. The mobility of hydrogen at low concentrations is presumably controlled by the deep sites. In fact, implantation experiments appear to suggest that atomic hydrogen may be highly mobile in the absence of lattice damages⁵⁰. Astrophysical grains are likely to be damaged. However, once the deep sites are filled the mobility of additional atomic hydrogen in the bulk could be large. The best value for the solution energy, according to ref.⁴⁴, is that given by Atsumi et al.⁵¹: $E_s = -0.2$ eV (cf. figure 1 case iv), and for the diffusion energy is $E_D = 2.8$ eV. The energy difference between the surface and bulk ground states is given by $E_e - E[H]^b = E_c - E_s$ (cf. §III D). With the values of E_c discussed above, $E_s = -0.2$ eV implies that this energy gap lies in the range between 1.3 and 2.1 eV. The condition on the maximum equilibrium abundance to prevent saturating the bulk is very strict on account of the large energy gap: $\theta_{sat} = g_s e^{-(E_c - E_s)/kT_g}$ (cf. eq. [30]). If molecule formation on the surface is efficient we require

$$\ln[n(\text{H})(\epsilon/\text{eV})^{1/2} d_{-8}^2 T(\epsilon)] < 54 - 30(z_o/\text{\AA}) \min\left(\frac{T_t}{T_g}, 1\right) - \frac{3 \times 10^4}{T_g} \left(\frac{E_c - E_s}{1.3\text{eV}}\right), \quad (60)$$

or if H evaporation dominates

$$\ln[n(\text{H})(\epsilon/\text{eV})^{1/2} d_{-8}^2 T(\epsilon)] < 54 - \frac{2.8 \times 10^4}{T_g} \left(\frac{E_e + E_c - E_s}{2.44\text{eV}}\right). \quad (61)$$

Neither condition can be satisfied for typical astrophysical conditions so H saturation is favored.

It is important to recognize that the surface to bulk exchange rate has a large typical activation energy $\Delta E = E_D + E_s - E_c$. For $E_D = 2.8$ eV, we obtain ΔE between 1.5 and 0.7 eV. Given these estimates we anticipate the surface to bulk exchange rate to be much smaller than H or quantum pair evaporation rate. Bulk saturation is achieved, however, if high energy particles penetrate the lattice.

This relatively simple picture for graphite could be complicated by the following additional chemical pathways. The bulk may avoid saturation in steady state if sufficiently rapid H_2 formation can occur in the bulk followed by rapid bulk to surface exchange of H_2 , or in the presence of rapid collisional transfer of bulk H to the surface.

Whether H_2 formation can take place in the bulk is unclear. It can be argued, based on the foregoing discussion, that if H_2 is stable in the bulk then the activation barrier for bulk to surface exchange of H_2 molecules is large (it must exceed that for H atoms; c.f figure 2) so that H_2 saturation is inevitable for the same reasons that H saturation is. In both cases, saturation of the deep binding sites could alter the effective interaction potential. By simply occupying the deepest sites, hydrogen within the grain may force newly added atoms or molecules to move amongst more weakly bound sites. Alternatively, completely new hydrogen interaction potentials may be relevant at high occupancies. In any case, the high abundance of H and/or H_2 can only be altered from that predicted previously if rapid migration to the surface of H or newly formed H_2 becomes possible. In fact, in refs.³⁶ it has been argued that there is strong indication of H_2 formation and migration in some forms of graphite and amorphous carbon films saturated with hydrogen. There is insufficient data to make a quantitative estimate of the rate for the latter process. It is likely, though, that once the bulk becomes saturated, then a newly intercepted atom in the bulk will either diffuse quickly to the surface where it evaporates or undergoes quantum pair recombination, as discussed above, or reside in the bulk long enough to recombine with another incident atom to form an H_2 molecule that will subsequently be ejected from the grain. The rates for these processes depend on the barriers of the shallow sites in the saturated bulk and the modified activation energy for bulk to surface transition. In all these more complicated scenarios, H_2 formation increases compared to the simple estimates based solely on pair evaporation. Thus, we conclude that at low enough grain temperatures effective H_2 formation should take place in or on these putative carbon grains.

VI. SUMMARY AND CONCLUSIONS

In this paper we have examined the conditions required for effective molecular hydrogen formation in and on solids, with particular emphasis on astrophysical grains.

Much of the earlier work has been concerned with the catalysis of H_2 formation by surfaces of grains in molecular clouds, where the grain and gas temperatures are very low. The key processes determining the rate of H_2 formation are then: sticking and retention of the gas-phase atoms, diffusion of H along the surface, recombination with another H atom, and ejection of the newly formed H_2 molecule. In these scenarios the chemisorption sites are taken to be saturated and hydrogen atoms and molecules are weakly bound to physisorption sites with binding energies on the order of a few times 10^{-2} eV². This path may apply to grains coated by overlayers of molecular material such as amorphous ice⁵². The evaporation time of H from these weak binding sites is very short even at the low grain

temperatures envisioned, but deeper (impurity) sites may retain a fraction of the H atoms for long enough time, and act as reaction sites². The migration time of a newly adsorbed H atom to a reaction site is typically very short compared with the residence time⁵³ (but c.f. ref.⁵²), so that the factors limiting the H₂ formation rate are the sticking probability and retention of H.

The mechanisms controlling the rate of molecular hydrogen formation on grains could be markedly different under harsher conditions, e.g., in the vicinity of an astrophysical shock. Firstly, the grain may be exposed to fluxes of energetic particles or intense UV/X radiation, and this may lead to surface cleaning, surface reshaping, lattice modification and so forth that create chemisorption sites. Secondly, the gas-phase atoms may be energetic enough to penetrate deep inside the grain and, under certain conditions, to drive direct collisional reactions. H₂ formation may then occur, (1) in the bulk via thermal activation, (2) in the bulk by direct recombination with incident H atoms, (3) on the surface by thermally activated recombination of chemisorbed H atoms, (4) by direct recombination of an incoming atom with a chemisorbed atom, and (5) through pair evaporation. In case 4 a fraction of the newly formed H₂ molecules may be ejected immediately from the grain, a possibility discussed earlier in ref.⁴⁶, and referred to here, following him, as prompt reaction. Chemisorption of hydrogen on carbon has been studied by several authors^{48,49}, who calculated interaction potentials and chemisorption energies of atomic hydrogen on ideal graphite surfaces using quantum chemical techniques. There remains some variation in these results, so we have treated the value of the binding energy as a parameter.

The efficiency of H₂ formation depends, quite generally, on the characteristics of the solid including the following energy scales: the ground state energies of H and H₂ in the bulk, surface and vacuum; the energy barriers for site to site diffusion, for surface to bulk exchange, for H₂ formation in the bulk, on the surface and for pair formation above the surface. The efficiency also depends on the grain temperature and the flux and energy (particularly if high enough to drive collisional reactions) of H nuclei impinging on the grain. It is important to remember that the energy levels and activation barriers themselves depend on the density of hydrogen in and on the solid by virtue of the self interaction of hydrogen atoms and molecules. These values could be altered substantially when the grain reaches saturation.

In this work we have explored various recombination reaction pathways that may operate under a wide range of conditions. By constructing simple analytic models, we identify the regimes in the space of physical parameters that correspond to *effective H₂ formation* and *grain saturation* by H atoms and H₂ molecules. Although our model is general we have focused on the case of “clean” grains with only one type of surface site and one type of bulk site. So, our examples do not apply to the classic molecule formation mechanism explored by Hollenbach and Salpeter⁵³ which envisioned two surface sites with different binding energies. We also assume that hydrogen diffusion in the bulk and on the surface is rapid enough to render the bulk and surface occupation probabilities homogeneous. The processes incorporated in our model include: thermally activated and collisionally induced exchange of H and H₂ between the bulk and the surface, H₂ formation in the bulk and on the surface by thermal activation and direct recombination with incoming atoms, pair evaporation, prompt reaction, thermal evaporation and collisional ejections and a variety of dissociation reactions in and on the solid (by thermal activation, by quantum tunneling and by direct collisions).

Despite the large number of physical parameters involved, the solutions for the H and H₂ bulk and surface concentrations and the H₂ formation efficiency are found to be highly degenerate, and depend only on a relatively small number of dimensionless parameters. In the following, we briefly summarize the main results for the three distinct cases we have considered: when H₂ forms from H atoms leaving the surface, when it also forms on the surface, and finally when it forms in the bulk.

If there are no bound H₂ states in the bulk and on the surface, H₂ formation occurs via pair evaporation or prompt reaction. Two cases are of interest. (a) In materials which have positive chemisorption energy, as appears to be the case for carbon, pair evaporation can proceed quantum mechanically even at zero temperature. Our result is that $\mathcal{E} > 0.5$ when $S((\Gamma_{2H}/g_s\Gamma_H^2)+2\alpha_{Fs}/\Gamma_H) > 1$. In the absence of collisions this is simply $-\ln(\Gamma_{2H}/\nu_o)-2E_e/kT_g-\ln(S/g_s\nu_o) < 0$ so that effective H₂ formation is “guaranteed” as long as the loss rate of atomic hydrogen by evaporation is less than the quantum pair evaporation rate. This is essentially a condition on the maximum grain temperature. (The threshold grain temperature does depend on the rate at which H nuclei are intercepted by the grain but the dependence is logarithmic and therefore weak.) If the grain temperature is large, the surface density of H is small and the efficiency of formation of H₂, which is a process quadratic in the surface density, is small. (b) For materials with negative chemisorption energy, binding to the surface of H is energetically favorable so that surface densities would saturate at typical grain temperatures. Pair evaporation and H evaporation both require thermal activation but generally molecule formation will proceed with more rapidity simply because H₂ is bound with respect to H in the vacuum. (We are assuming that the barrier to H₂ formation is less than the embedding energy of H.) For these materials, the efficiency of molecule formation will be high. However, since the overall loss rate is exponentially sensitive to temperature these materials will become saturated if the grain temperature is too low. Saturation of the surface occurs when $2\Gamma_{2H} + \Gamma_H < g_s^{-1}S$. Whenever grain saturation of the surface occurs it is possible that the important parameters describing the grain are modified.

For both materials above, collisional ejections of H atoms and prompt reaction may alter the results; the former releases atomic hydrogen from the grain and reduces the H₂ formation efficiency, whereas the latter leads to effectively higher surface recombination rate and, therefore, enhanced efficiency. The rates of both processes are independent of the grain temperature (to the extent that α_{Fs} and α_{sv} themselves do not depend on T_{gr}). As figure 3 illustrates, these processes can significantly alter the regimes of effective and ineffective H₂ formation and also grain saturation.

When H₂ can associate/dissociate and adhere to the grain surface (but not the interior) the above situation is more complicated. H₂ formation on the surface always increases the formation rate by pair evaporation alone [this is mathematically made clear by the simple modification needed for eqn. (31)]. The efficiency of molecule formation is increased. This qualitatively modifies our previous example only when formation would be otherwise inefficient. Efficient formation requires $\bar{t}_{Fs}^{-1} \gg g_s \Gamma_H^2 / S$, where \bar{t}_{Fs}^{-1} is the effective formation rate defined explicitly in eq. (29). The limiting cases were discussed and correspond to (1) H₂ formation followed by immediate evaporation from the surface and (2) evaporation of the surface equilibrium H₂ fraction. Numerically, efficiency contours are given by the modified form of eq. (33).

In so far as saturation is concerned, it is more difficult for H to saturate the surface. At the same time, surface formation also introduces the possibility that H₂ may become saturated on the surface if the release rate from the grain is not fast enough. The detailed conditions are given in eqn. (38).

H₂ production in the bulk requires the existence of bound H₂ states inside the solid, as depicted in figure 2. It is unknown which substances allow such bound states. If bound states exist, the process has many similarities to H₂ formation on the surface. Likewise, it increases the net efficiency. We have calculated the effect of bulk formation independent of the surface and pair evaporation processes. The H and H₂ occupation probabilities as well as the formation efficiency depend on the net rate of release of atomic and molecular hydrogen from the bulk and, consequently, involve the exchange rates between bulk and surface. The full solution for H and H₂ occupancies and the efficiency depends on 7 dimensionless parameters but the bulk concentration depends on only 2. Additional simplifications are possible if the transfer time of H from surface to bulk is very short or the injection rate of H into bulk sites exceeds that into surface sites. The latter case is particularly relevant for homogeneous injection, the limit achieved when high energy particles penetrate the lattice. We show that the bulk concentration of H may be simply expressed as a function of x_R and x_F (figure 5), where x_F is the ratio of bulk H₂ formation rate to injection rate per site, and x_R is the ratio of net release rate of H from the bulk to injection rate per site. The sensitivity of these results to the dissociation rate is also discussed (the ratio of H₂ dissociation rate and release rate of H₂ from the bulk is η). The domains of H and H₂ saturation are described.

H₂ formation within the bulk can proceed as a thermally activated reaction or by collisional impact of a high energy particle. If collisional H₂ formation is less important than thermally activated formation, then equilibrium is achieved between release and thermal formation. The efficiency depends on x_F/x_R^2 (see figure 6 and segment with slope 2). In the alternative limit, collisional formation achieves equilibrium with release (figure 6 with segment with slope 0). The location of the efficiency curves also depends on η . The efficiency is essentially independent of η when $\eta \ll 1$ and decreases as η increases for $\eta > 1$.

As an application we have considered H₂ formation on carbon. This system is complicated by virtue of the broad spectrum of binding sites exists in the solid. Despite this complication we were able to draw some general conclusions using results of simulations and data available in the literature. In particular, 1) efficient molecule formation requires grain temperatures smaller than about 100 K, 2) pair evaporation will keep the surface unsaturated even at very low grain temperatures if $n(H)(\epsilon/eV)^{1/2} < 2.5 \times 10^9 \text{ cm}^{-3}$ where $n(H)$ is the number density of gas phase atoms and ϵ is their average energy, and 3) the bulk will be saturated in steady state unless sufficiently rapid molecule formation will take place in the bulk followed by rapid transfer of H₂ to the surface or if the incident atoms are energetic enough to eject bulk H to the surface at a large enough rate.

ACKNOWLEDGMENTS

D.F. Chernoff thanks Chris McKee for stimulating conversations which motivated this work. We acknowledge helpful discussions with Neil Ashcroft, Barbara Cooper, Tatjana Čurčić, Bruce Roberts and Mike Teter. This work was supported by an Alon fellowship (AL) and at Cornell University by NSF grant AST-9530397 and NASA grant NAGW-5-2851.

- ¹ Present address: School of Physics and Astronomy, Tel Aviv Univ., 69978 Tel Aviv, Israel
- ² D. Hollenbach, & E.E. Salpeter, *Astrophys. J.*, **163**, 155 (1971); W.D. Watson, & E.E. Salpeter, *Astrophys. J.*, **174**, 321 (1972)
- ³ T.N. Gautier, U. Fink, R.R. Treffers, & H.P. Larson, *Astrophys. J.* **207**, L129 (1976); S. Beckwith, S.E. Persson, G. Neugebauer, & E.E. Becklin, *Astrophys. J.* **223**, 464 (1978); N.Z. Scoville, D.N.B. Hall, S.G. Kleinmann, & S.T. Ridgway, *Astrophys. J.* **253**, 136 (1982); D. Nadeau, T.R. Geballe, & G. Neugebauer, *Astrophys. J.* **253**, 154 (1982); S. Beckwith, N.J. Evans, I. Gatley, G. Gull, & R.W. Russell, *Astrophys. J.* **264**, 152 (1983); P.W.J.L. Brand, A. Moorhouse, M.G. Burton, T.R. Geballe, M. Bird, & R. Wade, *Astrophys. J.* **334**, L103 (1988)
- ⁴ M.G. Burton, P.W.J.L. Brand, T.R. Geballe, & A.S. Webster, *Astrophys. J.* **236**, 409 (1989)
- ⁵ R.R. Treffers, *Astrophys. J.* **233**, L17 (1979); M.G. Burton, T.R. Geballe, P.W.J.L. Brand, & A.S. Webster, *Astrophys. J.* **231**, 617 (1988)
- ⁶ J.R. Graham, G.S. Wright, J.J. Hester, & A.J. Longmore, *Astron. J.* **101**, 175 (1991)
- ⁷ W.J. Zealey, P.M. Williams, & G. Sandell, *Astron. & Astrophys.* **140**, L31 (1984)
- ⁸ J. Fischer, T.R. Geballe, H.A. Smith, M. Simon, & J.W.V. Storey, *Astrophys. J.* **320**, 667 (1987)
- ⁹ J. Fischer, M. Simon, J. Benson, & P.M. Solomon, *Astrophys. J.* **273**, L27 (1983)
- ¹⁰ B. Draine, & E.E., Salpeter, *Astrophys. J.*, **231**, 77 (1979)
- ¹¹ H.H. Dunker & V.I. Lygin, *Quantenchemie der Adsorption an Festkörperoberflächen*, Leipzig (1978)
- ¹² L. Spitzer, *Physical Processes in the Interstellar Medium*, New York: Wiley (1978)
- ¹³ C.F. McKee, D. Hollenbach, C.G. Seab, & A.G.G.M. Tielens, *Astrophys. J.*, **318**, 674 (1987)
- ¹⁴ D. Hollenbach, & C.F. McKee, *Astrophys. J. Supp.*, **41**, 555 (1979)
- ¹⁵ B.T. Draine, *Physics of the Interstellar Medium and Intergalactic Medium*, eds. A. Ferrara, C.F. McKee, C. Heiles and P.R. Shapiro, p. 133, San Francisco: ASP (1994)
- ¹⁶ E.E. Salpeter, *Phys. Rev. Lett.*, **28**, 560 (1972)
- ¹⁷ M. I. Baskes, *J. Nucl. Mater.*, **128**, 676 (1984); J.W. Cuthbertson, W.D. Langer, & R.W. Motley, *J. Nucl. Mater.*, **196-198**, 113 (1992); D.M. Goodstein, S.A. Langer, & B. Cooper, *J. Vac. Sci. Technol. A*, **6**, 703 (1988)
- ¹⁸ W. Eckstein, & J.P. Biersack, *Appl. Phys. A.*, **38**, 123 (1985)
- ¹⁹ A.D. Tenner, R.P. Saxon, K.T. Gillen, D.E. Harrison, T.C.W. Horn, & A.W. Kleyn, *Surf. Sci.* **172**, 121 (1986); D.M. Goodstein, R.L. McEachern, & B. Cooper, *Phys. Rev. B.*, **39**, 13129 (1989)
- ²⁰ D.L. Adler, & B. Cooper, *Phys. Rev. B*, **43**, 3876 (1991)
- ²¹ J.P. Biersack, & W. Eckstein, *Appl. Phys.*, **34**, 73 (1984)
- ²² R.I. Masel, in *Principles of Adsorption and Reaction on Solid Surfaces*, New York: John Wiley (1996)
- ²³ C.A. DiRubio, Ph.D. Thesis, Cornell Univ. (1993)
- ²⁴ G.A. Beitel, *J. Vac. Sci. Technol.* **6**, 224 (1969)
- ²⁵ J.F. Ziegler, J.P. Biersack, & U. Littmark, *The Stopping and Range of Ions in Solids*, New York: Pergamon (1985)
- ²⁶ H.M. Urbassek, in *Interaction of Charged Particles with Solids and Surfaces*, eds. A. Gras-Marti et al., p. (1991)
- ²⁷ L. Leblanc, & G.G. Ross, *Nucl. Instr. and Meth.* **83**, 15 (1993)
- ²⁸ F. Ruette (ed.), *Quantum Chemistry Approachs to Chemisorption and Heterogenous Catalysis*, Kluwer Academic Publishers (1992)
- ²⁹ I. Nagy, B. Apagyi, & K. Ladanyi, in *Interaction of Charged Particles with Solids and Surfaces*, eds. A. Gras-Marti et al., p. (1991); P.M. Echenique, & M.E. Uranga, in *Interaction of Charged Particles with Solids and Surfaces*, eds. A. Gras-Marti et al., p. 39 (1991)
- ³⁰ K. Christmann, *Surface Sci. Rep.*, **9**, 1 (1988)
- ³¹ C. Schermann, et al., in *Molecules and Grains in Space*, ed. Irene Nenner, AIP, pp. 801 (1994)
- ³² K.L. Wilson, in *Data Compendium for Plasma-Surface Interactions*, *Nucl. Fusion*, special issue, pp. 28 (1984)
- ³³ W. Moller, & J. Roth, in *Physics of Plasma-Wall Interactions in Controlled Fusion*, eds. D.E., Post, and R. Behrisch, NATO ASI, pp. 439 (1986)
- ³⁴ M.S. Daw, & S.M. Foiles, *Phys. Rev. B.*, **35**, 2128 (1987)
- ³⁵ Y. Shirasu, S. Yamanaka, & M. Miyake, *J. Nucl. Mater.*, **200**, 218 (1993)
- ³⁶ W. Moller, & B.M.U. Scherzer, *Appl. Phys. Lett.*, **50**, 1870 (1987); W. Moller, *J. Nucl. Mater.*, **162-164**, 138 (1989); H. Sugai, S. Yoshida, & H. Toyoda, *App. Phys. Lett.*, **54**, 1412 (1989)
- ³⁷ C.Y. Lee, & A.E. DePristo, *J. Chem. Phys.*, **84**, 485 (1985)
- ³⁸ S.M. Foiles, M.I. Baskes, C.F. Melius, & M.S. Daw., *J. Less-Common Metals*, **130**, 465 (1987)
- ³⁹ A.V. Hamza, & R.J. Madix, *J. Phys. Chem.*, **89**, 5381 (1985); H.J. Robota, et al., *Surface Sci.*, **155**, 101 (1985)
- ⁴⁰ J. Harris, & S. Andersson, *Phys. Rev. Lett.*, **55**, 1583 (1985); P. Madhavan, & J.L. Whitten, *J. Chem. Phys.*, **77**, 2673 (1982)
- ⁴¹ J.K. Norskov, et al., *Phys. Rev. Lett.*, **46**, 257 (1981)
- ⁴² K.W. Kehr, in *Hydrogen in Metals I*, eds. G. Alefeld, & J. Völkl, p. 197 (1978)
- ⁴³ J. Völkl, & G. Alefeld, in *Hydrogen in Metals I*, eds. G. Alefeld, & J. Völkl, p. 321 (1978)
- ⁴⁴ A. Causey, *J. Nucl. Mater.*, **162-164**, 151 (1989)
- ⁴⁵ A. Auerbach, K.F. Freed, & R. Gomer, *J. Chem. Phys.*, **86**, 2356 (1987)
- ⁴⁶ W.W. Duley, *Mon. Not. R. Astro. Soc.*, **223**, 177 (1996)

- ⁴⁷ R.M. Barrer, Proc. Roy. Soc., **149A**, 253 (1935); R.C. Bansal, F.J. Vastola, & P.L. Walker Jr., Carbon, **9**, 185 (1971)
- ⁴⁸ S. Aronowitz, & S. Chang, Astrophys. J., **293**, 243 (1985); A.J. Bennett, B. McCarroll, & R. Messmer, Surf. Sci., **24**, 191 (1971); R. Dovesi, C. Pisani, & C. Roetti, Chem Phys. Lett., **81**, 498 (1981);
- ⁴⁹ S. Klose, Astron. nachr., **310**, 409 (1989)
- ⁵⁰ P. Hucks, K. Flaskamp, & E. Vietzke, J. Nucl. Mater., **93-94**, 558 (1980); K. Sone, & G.M. McCracken, J. Nucl. Mater., **111-112**, 606 (1982)
- ⁵¹ H. Atsumi, S. Tokura, & M. Miyake, J. Nucl. Mater **155-157**, 241 (1988)
- ⁵² V. Buch, & Q. Zhang, Astrophys. J., **379**, 647 (1991); R. Smoluchowski, J. Phys. Chem., **87**, 4229 (1983)
- ⁵³ D. Hollenbach, & E.E. Salpeter, J. Chem. Phys., **53**, 79 (1970)

FIGURE CAPTIONS

FIG. 1. Schematic energy diagrams of hydrogen in solids for which no bound H_2 states exist in the bulk and on the surface. The solid curve represents the interaction potential of a single H atom with the solid. The two dashed lines represent the interaction potential of an atom pair; one dashed line corresponds to a pair at fixed interatomic distance of order that of a free H_2 molecule, and the other to a minimum energy configuration. The chemisorption energy, E_c , solution energy, E_s , activation energy of chemisorption, E_a , activation energy of pair evaporation, E_r , and dissociation energy of H_2 in vacuum per H atom are indicated. The sign of E_c and E_s is defined by the direction of the corresponding arrows; positive if the arrow points upwards and negative if it points downwards. The four cases shown correspond to different possible ordering of the energy levels (see text for detailed discussions).

FIG. 2. The same as figure 1, but in the case in which H_2 is stable in and on the solid. The thick arrows indicate different pathways for H_2 formation and release: [1] H_2 formation in the bulk, [2] H_2 formation on the surface, [3] pair evaporation, and [4] evaporation of H_2 from the surface. Each reaction may involve an activation barrier as shown schematically.

FIG. 3. Domains of grain saturation, effective and ineffective H_2 formation for materials for which there are no bound H_2 states on the surface and in the bulk, in the absence of (windows a and b) and in the presence of (windows c, d) collisional reactions. The independent variables are the log of pair evaporation rate per attempt frequency, Γ_{2H}/ν_o , and the embedding energy in units of the grain temperature E_e/kT_g .

FIG. 4. Conditions for effective and ineffective H_2 formation for specific materials. The dashed line corresponds to embedding energy $E_e = 2.55$ eV, chemisorption energy $E_c = -0.3$ eV, activation energy of chemisorption $E_a = 0.2$ eV, and barrier penetration depth $G_H > 7$, and represents a typical transition metal. The dotted-dashed line corresponds to $E_c > 0$, $E_e = 0.3$ eV, activation energy of pair evaporation $E_r = 0.4$ eV, and $G_H = 30$, and represents carbon (see example in §V).

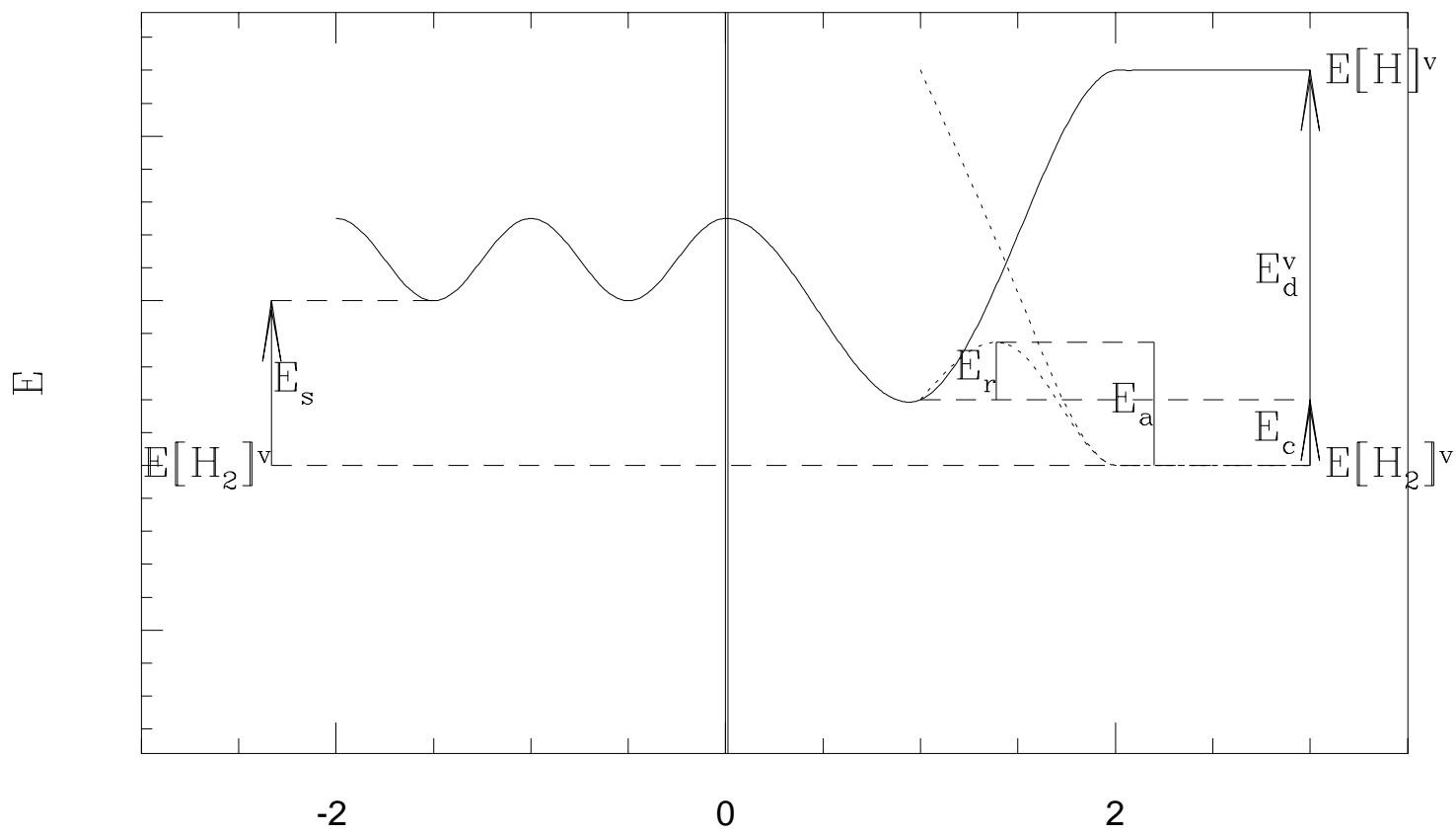
FIG. 5. n_H contours plotted in the plane defined by x_F - the ratio of thermally activated H_2 formation rate in the bulk and injection rate per site, and x_R - the net release rate per H atom of bulk atomic hydrogen in units of the injection rate per site, for $\alpha_{Fb} = 0$, $\eta = 0$ (solid lines) and $\eta = 10^2$ (dotted lines). Values of n_H label the curves. The curve separating the regimes of saturated and unsaturated grain is shown schematically (dashed line).

FIG. 6. Contours of H_2 formation efficiency, \mathcal{E} , for $\eta = 0$, $\alpha_{Fb} = 0$ (solid lines) and $\alpha_{Fb} = 10^2$ (dashed lines). The efficiency curves are broken power laws (see eq. [55]). The change in slope reflects the transition from the regime where thermally activated H_2 formation dominates to the regime where collisional recombination of a bulk H atom with an incoming atom dominates.

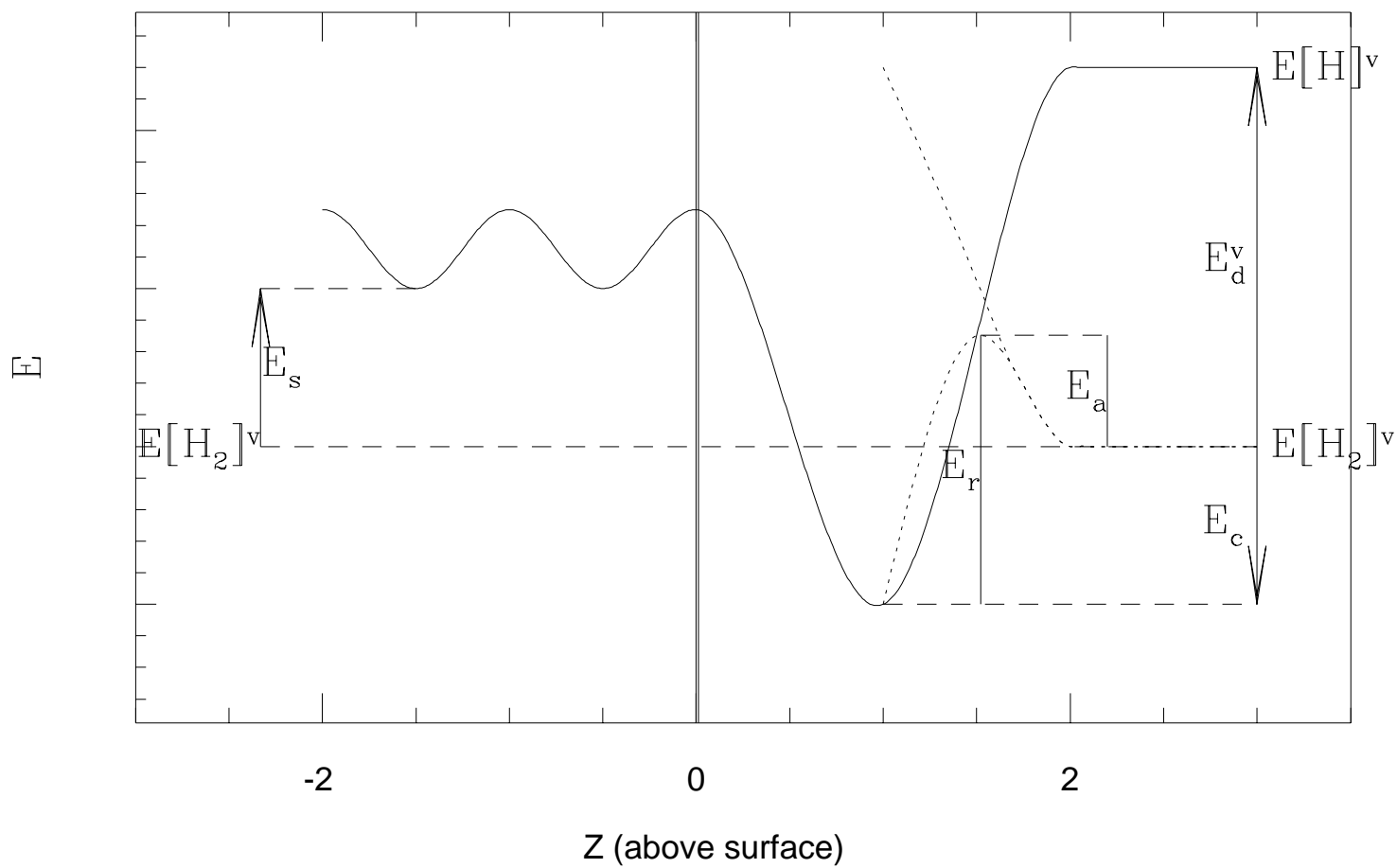
APPENDIX: LIST OF SYMBOLS

- T_g - Grain temperature
 T_t - Tunneling temperature
 n_X - Fraction of all sites occupied by species X in the bulk; ($X = \text{H}, \text{H}_2$)
 θ_X - Fraction of all sites occupied by species X on the surface; ($X = \text{H}, \text{H}_2$)
 \mathcal{N} - Total number of sites
 g_b - Ratio of the number of bulk sites and \mathcal{N}
 g_s - Ratio of the number of surface sites and \mathcal{N}
 S - Total injection rate per site
 S_H - Injection rate per site into bulk sites
 S_H - Injection rate per site into surface sites
 \mathcal{E} - H_2 formation efficiency
 $E[X]^i$ - Ground state energy of species X ; ($X = \text{H}, \text{H}_2, i = b, s, v$)
 E_c - Chemisorption energy
 E_e - Embedding energy
 E_s - Solution energy
 E_d^i - Dissociation energy; ($i = b, s, v$)
 E_r - Activation energy of pair evaporation
 E_a - Activation energy of chemisorption
 G_H - Penetration factor for quantum pair evaporation
 t_{in} - Mean time for particle interception by the grain
 t_{Fi} - Thermally activated H_2 formation time; ($i = b, s$)
 t_{Di} - Thermally activated H_2 dissociation time; ($i = b, s$)
 t_{Fsb} (t_{Fbs}) - Time of H_2 formation in the bulk (on the surface) by thermally activated recombination of surface and subsurface atoms
 t_{Dbs} (t_{Dsb}) - Time of H_2 dissociation in the bulk (on the surface) to produce a surface and subsurface H
 t_{sbX} (t_{bsX}) - Time of thermally activated diffusion of a species X from the surface (bulk) to the bulk (surface)
 α_{Fi} - Probability per site of direct collisional recombination with an incoming H atom; ($i = b, s$)
 α_{svX} - Probability per site of collisional ejection of a species X
 β_i - Probability per site of collisional dissociation of an H_2 molecule; ($i = b, s$)
 γ_X - Thermal evaporation rate of a species X from the surface
 Γ_X - Total loss rate of a species X from the surface (sum of thermal evaporation and collisional ejection)
 Γ_{2H} - Pair evaporation rate
 q - Fraction of collisional dissociations on the surface that results in the immediate loss of the H atoms
 δ_{Fs} - Fraction of H_2 molecules formed by collisional recombination on the surface that remain on the surface

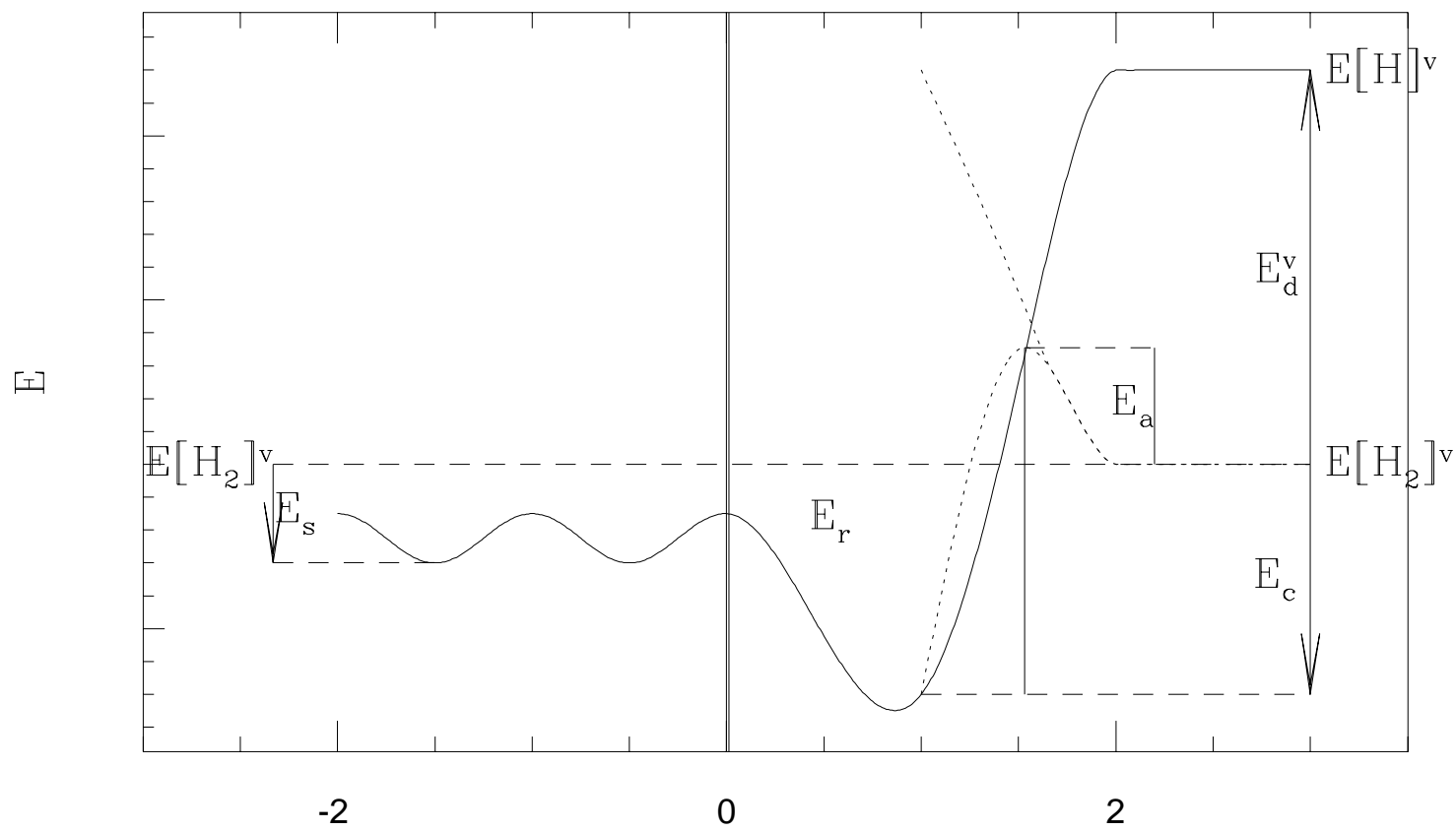
(i) $0 < E_c < E_s$



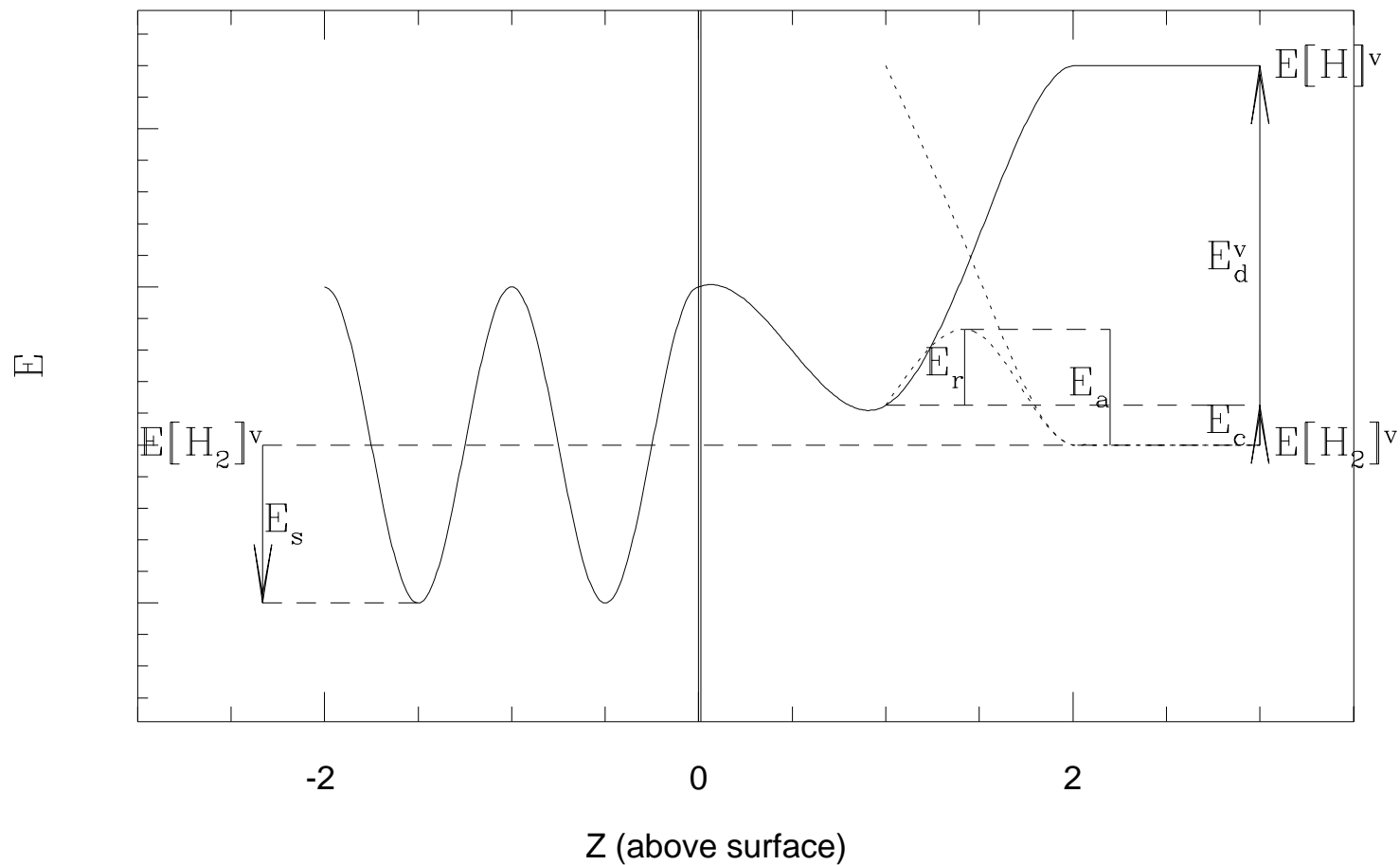
(ii) $E_c < 0 < E_s$

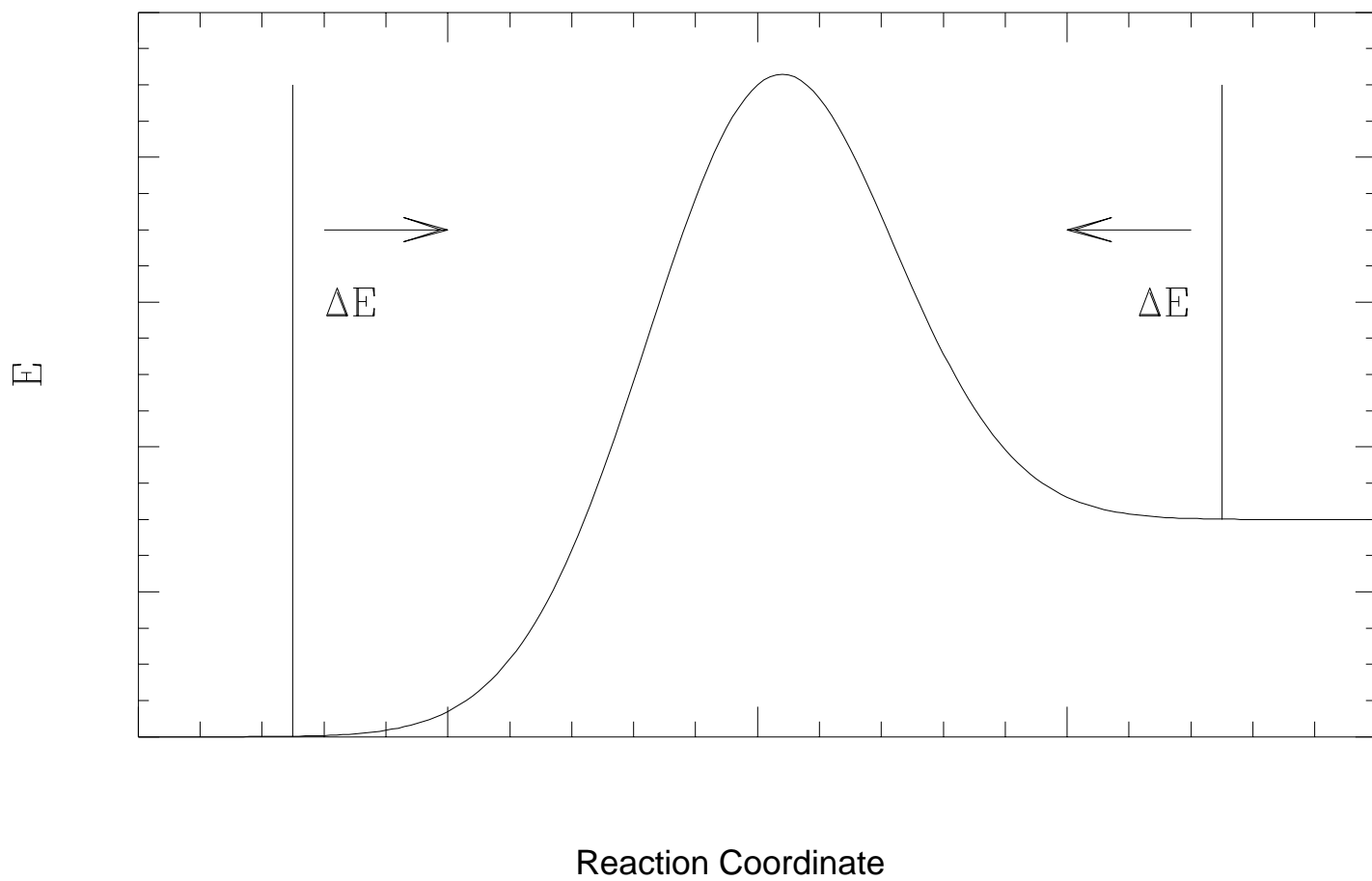
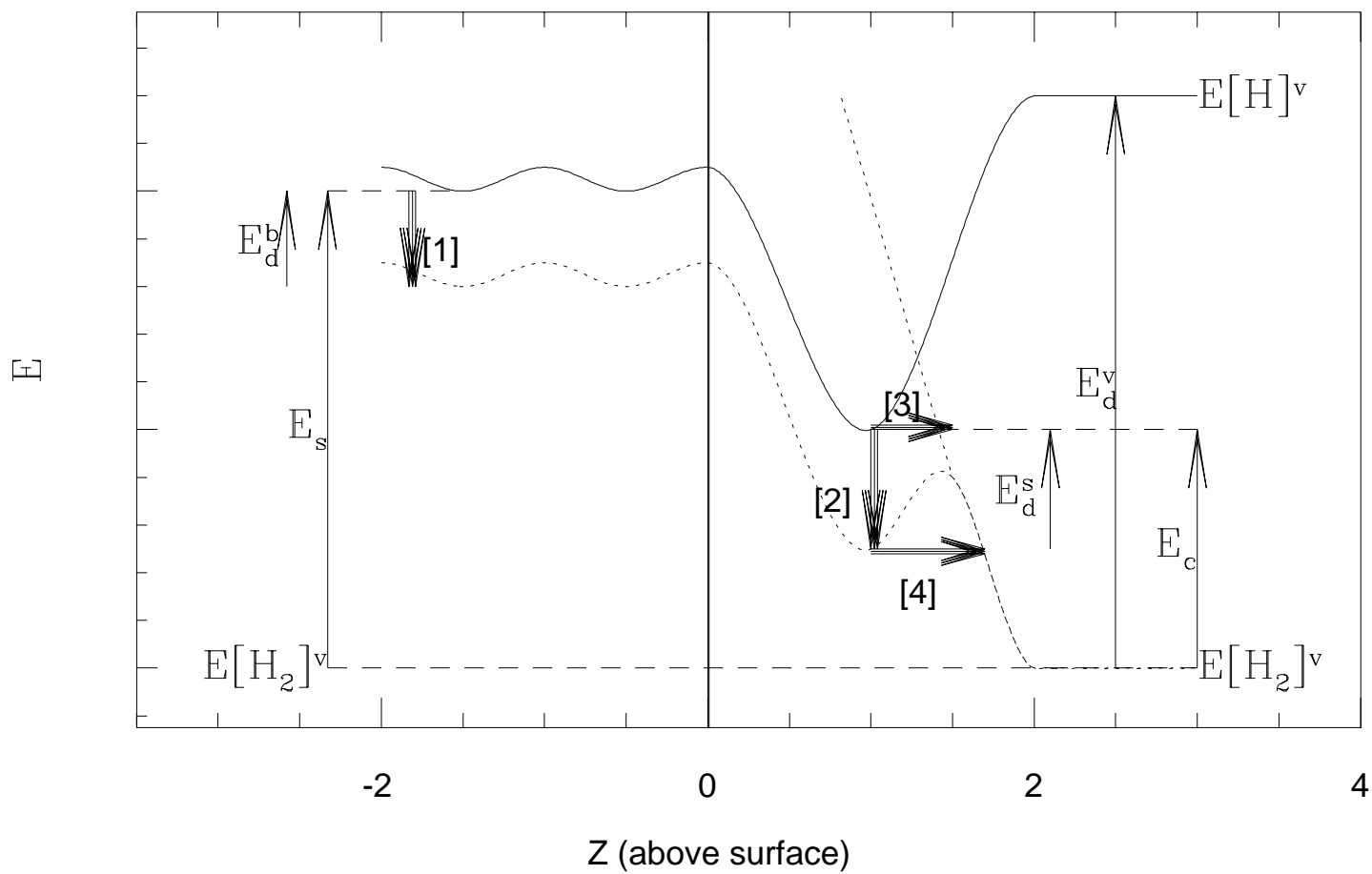


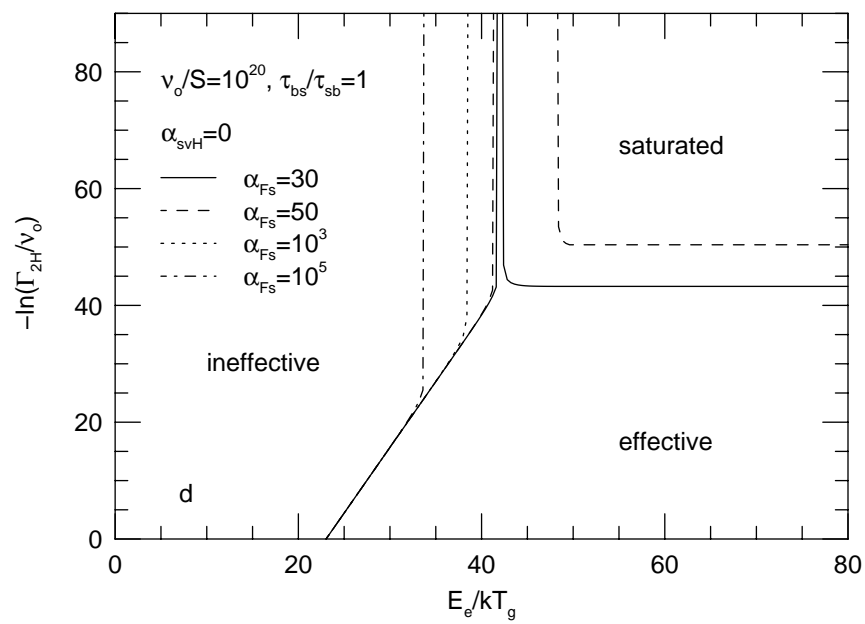
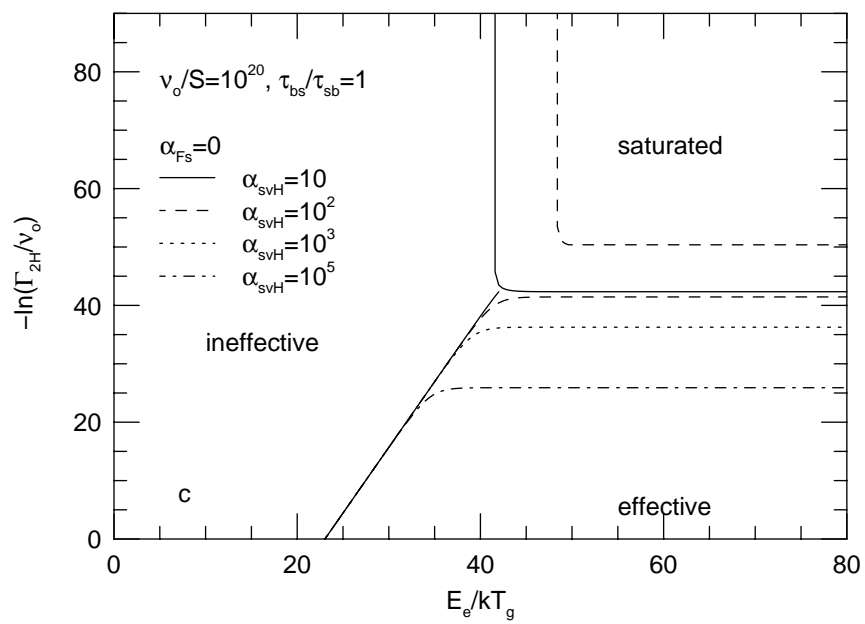
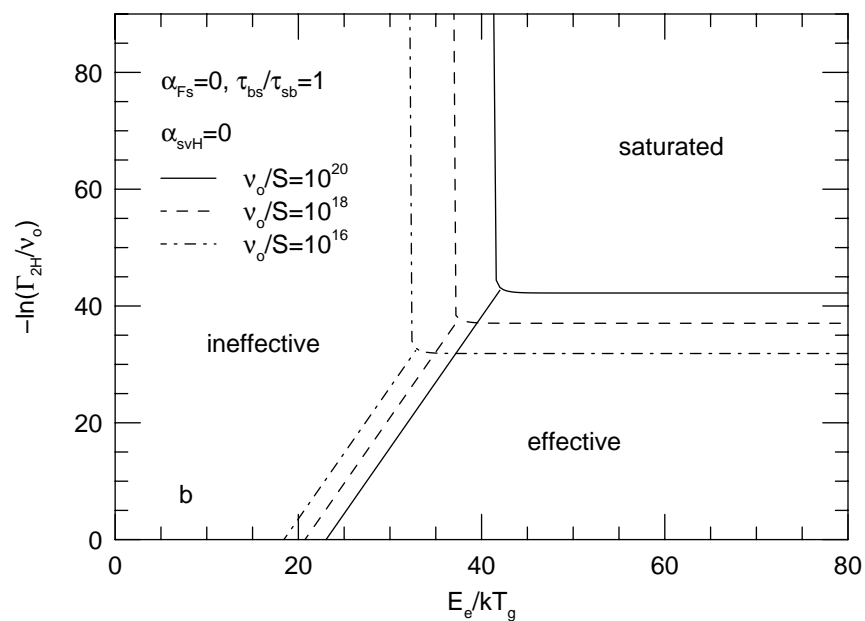
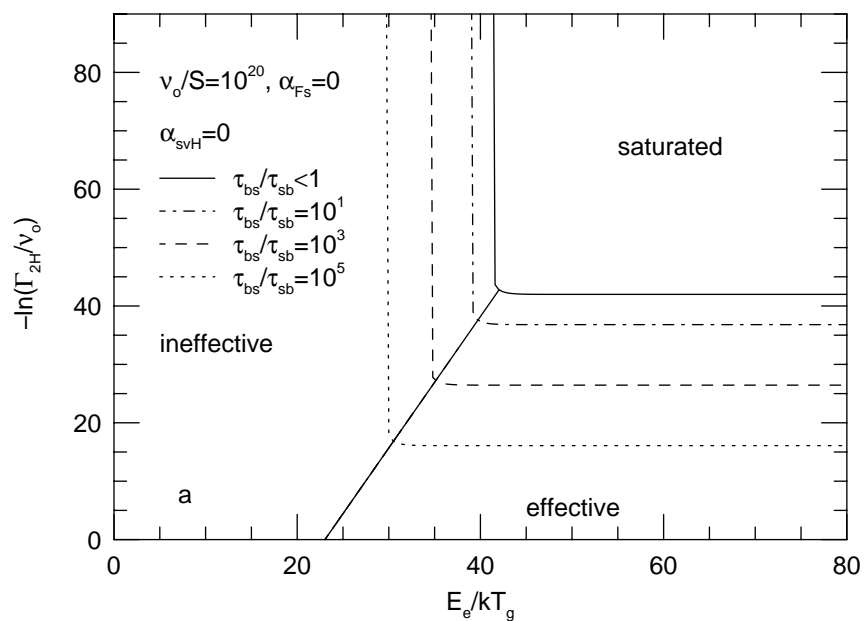
(iii) $E_c < E_s < 0$

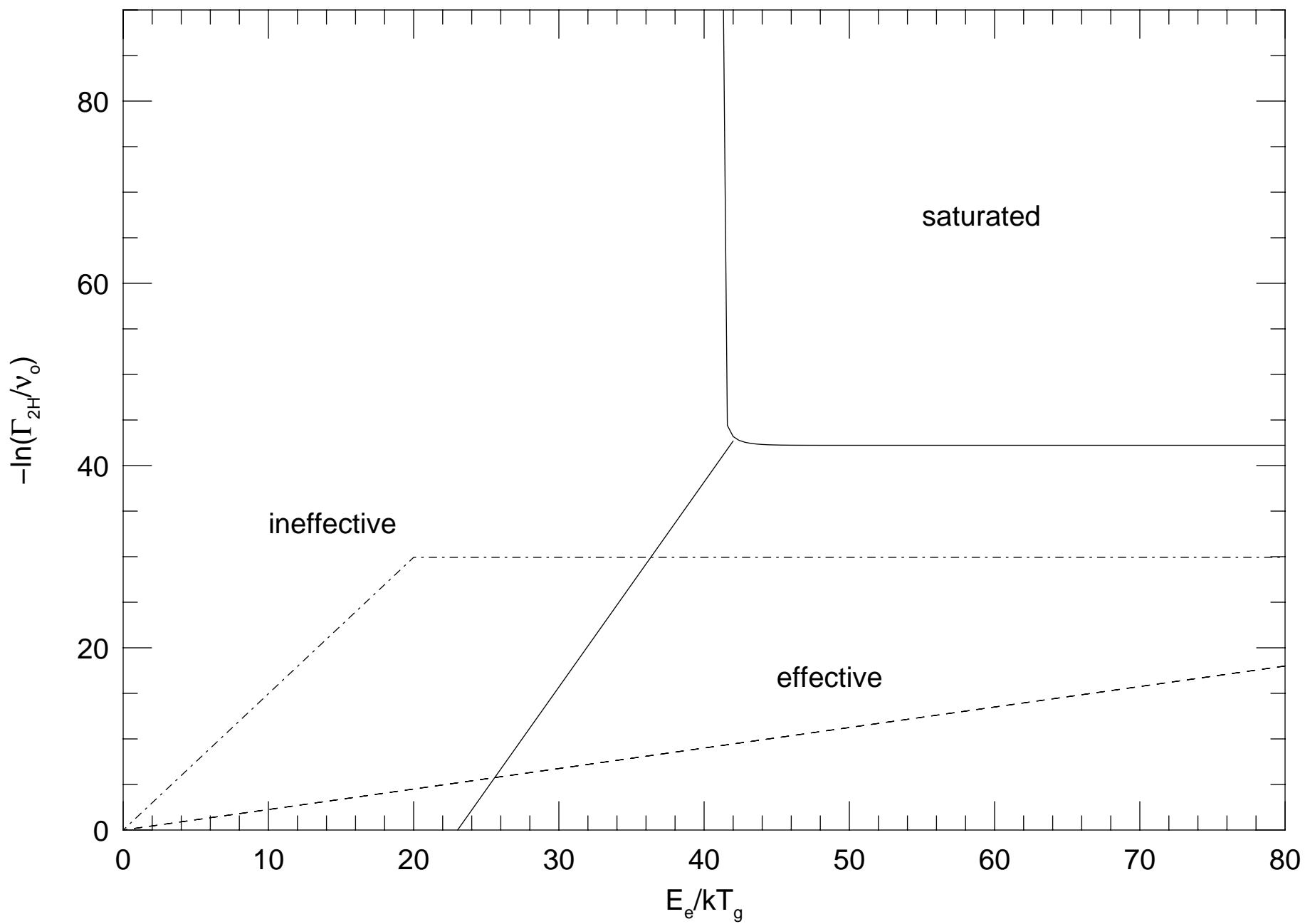


(iv) $E_s < 0 < E_c$

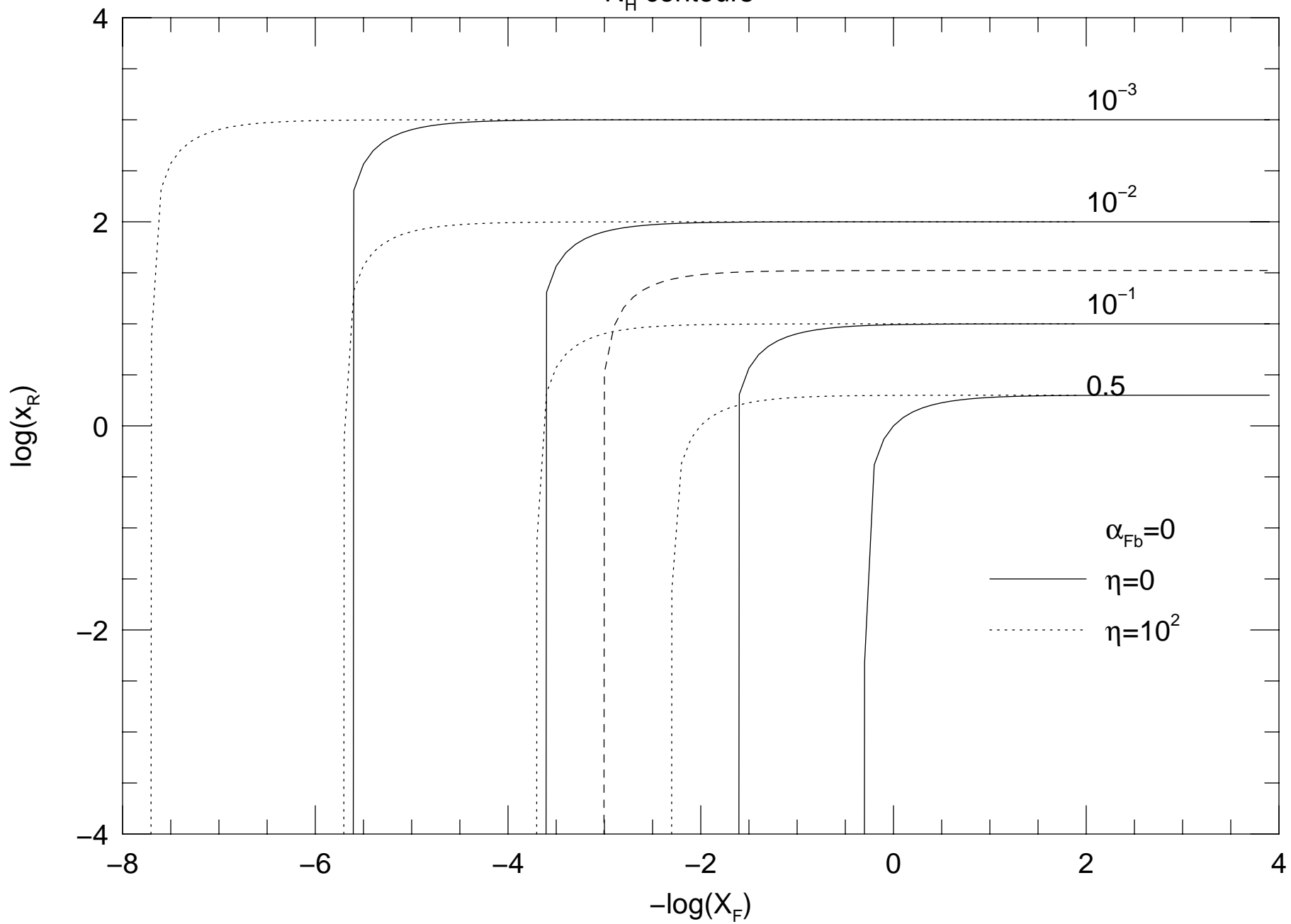








N_H contours



Efficiency contours

